Near critical, self-similar, blow-up solutions of the generalised Korteweg-de Vries equation: asymptotics and computations

Amodio, P.; Budd, C.J.; Koch, O.; Rottschäfer, V.; Settanni, G.; Weinmueller, E.

Physica D 401 (2020) 132179

Contents lists available at ScienceDirect

Physica D

journal homepage: www.elsevier.com/locate/physd

Near critical, self-similar, blow-up solutions of the generalised Korteweg–de Vries equation: Asymptotics and computations

Pierluigi Amodio [a], Chris J. Budd [b], Othmar Koch [c,*], Vivi Rottschäfer [d], Giuseppina Settanni [a], Ewa Weinmüller [e]

[a] Universitá degli Studi di Bari, Dipartimento di Matematica, Italy
[b] University of Bath, Mathematical Sciences, United Kingdom
[c] Universität Wien, Institut für Mathematik, Austria
[d] Leiden University, Mathematical Institute, Netherlands
[e] Technische Universität Wien, Institut für Analysis und Scientific Computing, Austria

ARTICLE INFO

Article history:
Received 18 December 2018
Received in revised form 26 June 2019
Accepted 26 August 2019
Available online 4 September 2019
Communicated by B. Sandstede

Keywords:
Generalised Korteweg–de Vries equation
Blow-up solutions
Asymptotic analysis
Numerical methods

ABSTRACT

In this article we give a detailed asymptotic analysis of the near critical self-similar blowup solutions to the Generalised Korteweg–de Vries equation (GKdV). We compare this analysis to some careful numerical calculations. It has been known that for a nonlinearity that has a power larger than the critical value $p = 5$, solitary waves of the GKdV can become unstable and become infinite in finite time, in other words they blow up. Numerical simulations presented in Klein and Peter (2015) indicate that if $p > 5$ the solitary waves travel to the right with an increasing speed, and simultaneously, form a similarity structure as they approach the blow-up time. This structure breaks down at $p = 5$. Based on these observations, we rescale the GKdV equation to give an equation that will be analysed by using asymptotic methods as $p \to 5^+$. By doing this we resolve the complete structure of these self-similar blow-up solutions and study the singular nature of the solutions in the critical limit. In both the numerics and the asymptotics, we find that the solution has sech-like behaviour near the peak. Moreover, it becomes asymmetric with slow algebraic decay to the left of the peak and much more rapid algebraic decay to the right. The asymptotic expressions agree to high accuracy with the numerical results, performed by adaptive high-order solvers based on collocation or finite difference methods.

1. Introduction

1.1. Overview

In this article, we study solutions that blow up in finite time of the Generalised Korteweg–de Vries (GKdV) equation of the following form

$$\frac{\partial \phi}{\partial t} + \frac{\partial}{\partial x}\left(\frac{\partial^2 \phi}{\partial x^2} + \phi^p\right) = 0, \tag{1}$$

where $\phi, x \in \mathbf{R}$, $t > 0$, and p is a positive parameter. Eq. (1) is subject to the initial condition

$$\phi(x, 0) = \phi_0(x).$$

We perform a careful asymptotic analysis of these solutions to reveal their structure and compare these with results from an equally careful numerical study. Our interest lies in those solutions which blow up at the single point $\tilde{x}$ in a finite time $T < \infty$ so that

$$\max_x |\phi(x, t)| \to \infty \text{ as } t \uparrow T,$$

with $|\phi(x, t)| < \infty$ for all $t < T, x \in \mathbf{R}$. In [1] it has been shown for Eq. (1) that for $p > 5$, and p close to $p = 5$, there exists a stable self-similar solution of the form

$$\phi(x, t) = (T - t)^{-2/3(p-1)} w(\xi), \quad \xi = \frac{(x - \tilde{x})}{(T - t)^{1/3}}. \tag{2}$$

We will establish very precise asymptotic estimates on the spatial structure of the function $w(\xi)$ as $p \to 5^+$, and we will verify these through some very careful numerical computations (which have to cope with very large local changes in the solution). These numerical calculations show excellent agreement with the asymptotic approximations in the limit of $p \to 5^+$ despite exponentially small behaviour of the solution tails in this limit.

* Corresponding author.
E-mail addresses: pierluigi.amodio@uniba.it (P. Amodio), mascjb@bath.ac.uk (C.J. Budd), othmar@othmar-koch.org (O. Koch), vivi@math.leidenuniv.nl (V. Rottschäfer), giuseppina.settanni@uniba.it (G. Settanni), e.weinmueller@tuwien.ac.at (E. Weinmüller).

https://doi.org/10.1016/j.physd.2019.132179
0167-2789/

1.2. Background

The GKdV equation (1) arises in modelling the propagation of small-amplitude waves in a variety of nonlinear dispersive media, where ϕ represents the wave amplitude, see [2,3]. Moreover, the equation also describes the behaviour of longitudinal waves propagating in a one-dimensional lattice of equal masses coupled by nonlinear springs; the Fermi, Pasta, Ulam (FPU)-lattice, see [4] and references therein. Together with the nonlinear Schrödinger equation, Eq. (1) can be considered as a universal model for Hamiltonian systems in infinite dimensions.

The special case $p = 2$ gives the classical Korteweg–de Vries equation (KdV) which was posed by Korteweg and de Vries [5] to describe water waves on shallow water. The case $p = 3$, which is known as the Modified Korteweg–de Vries equation, can be transformed into the original Korteweg–de Vries equation by the Miura transformation [6]. The case $5 < p \in \mathbb{N}$ is treated in [7], which addresses the approximation of the full PDE.

Eq. (1) is Hamiltonian, and there is conservation of the energy which is given by

$$\begin{aligned} E(\phi(t)) &= \frac{1}{2}\int_{\mathbf{R}}\left[\phi_x(x,t)^2 - \frac{1}{p+1}\phi(x,t)^{p+1}\right]dx \\ &= \frac{1}{2}\int_{\mathbf{R}}\left[\phi_x(x,0)^2 - \frac{1}{p+1}\phi(x,0)^{p+1}\right]dx < \infty. \end{aligned} \tag{3}$$

Moreover, the mass, given by

$$M(\phi(t)) = \int_{\mathbf{R}}\phi(x,t)^2 dx = \int_{\mathbf{R}}\phi(x,0)^2\, dx \tag{4}$$

is also conserved.

For $p = 2$ and $p = 3$ Eq. (1) is integrable and the solutions have been studied extensively analytically, see for example [8] and [9]. Moreover, for $p < 5$ all solutions in $H^1(\mathbf{R})$ are global and bounded in time as a result of the Gagliardo–Nirenberg inequality. For $p \geq 5$ the conservation laws (3) and (4) do not imply a bound in $H^1(\mathbf{R})$, uniform in time, for all H^1-solutions, and thus no global existence can be guaranteed. From this observation, the existence of solutions which blow up in finite time is suspected, and observed numerically, for $p \geq 5$. Here $p = 5$ is the so-called *critical power*.

Blow-up solutions can arise when a solitary wave becomes unstable, and hence, the study of stability of the solitary waves is a first step towards analysing blow-up behaviour. For all $p \geq 2$, explicit solitary waves of the GKdV equation are known,

$$\phi(x,t;C,x_0) = \left(\frac{p+1}{2}\, C\, \operatorname{sech}^2\left(\frac{p-1}{2}\sqrt{C}(x - x_0 - Ct)\right)\right)^{\frac{1}{p-1}}, \tag{5}$$

where $C > 0$ is the wave speed and x_0 a translation parameter. For $p = 2, 3, 4$, this family of solutions is known to be (asymptotically) stable with respect to perturbations [10]. For $p \geq 5$, even weaker statements of stability, such as orbital stability, are known to be false, [11]. Thus, $p = 5$ is also the critical case for the stability of the soliton solutions. A first numerical approach to try and understand stability and instability of solitons was taken in [12]. The instability manifests itself in blow-up in finite time; perturbations of solitary waves form a similarity structure which in turn blows up. In [13], a thorough numerical study was conducted to detect the exact structure of the blow-up solutions. Moreover, an asymptotic statement (for $|x| \to \infty$) about the structure and its self-similar form was made. However, the structure of the solution close to the point where it blows up was not studied there. Analytically, the H^1-instability of solitons for the supercritical case $p > 5$ was considered in [11], see also references therein, and [14] for the choice $p = 5$. In [15], a large set of initial data was obtained which lead to instability of the soliton solutions for $p \geq 5$. There, it was expected that these solutions actually blow up. Thereafter, the same authors analysed the blow-up of solutions in a series of articles for the critical case $p = 5$. In those articles, solutions in the energy space $H^1(\mathbf{R})$ are analysed. These works start with [16] where the existence of solutions that blow up in finite or infinite time in H^1 was proved for $p = 5$. Then, in [17] an upper bound on the blow-up rate was established. Moreover, a restriction on initial conditions such that blow-up in finite time occurs was determined there. Finally, in [18] the question of the blow-up profile, i.e. the asymptotic form of the solutions after rescaling, was studied. There, the authors prove that, for certain initial data, the solution converges at the blow-up time T, to a self-similar travelling solution with a universal profile that is local in space.

The recent works of Koch and Lan [1,19] have proved the existence of a stable self-similar solution when $p > 5$ including the limit of $p \to 5^+$. Numerical studies of the time dependent problem are given, for example, in the recent paper by Klein and Peter [7]. Here, we extend the above works by performing a very careful formal asymptotic analysis combined with a numerical study of the profile of the blow-up solutions of Eq. (1) for $p > 5$ and $p - 5 \ll 1$.

In particular, we determine the precise form of the blow-up profile for $p - 5 \ll 1$ both close to the peak of the solution and in the tails. In the case of $p = 6 -$ so not close to $p = 5 -$ a numerical calculation of the profile is given in [7], Figures 18 and 26. Our analysis does explain and confirm this profile shape. Especially, our analysis shows why the solution has the non-symmetric form: this is due to a remarkable difference in the behaviour in the tails. It turns out that the right-hand tail is exponentially small, in terms of $p - 5$, whereas the left-hand tail is algebraically decaying.

Furthermore, as $p \to 5^+$ the solution profile becomes very singular , with extremely rapid changes close to the peak and the very small size of the right-hand tail as $\xi \to +\infty$. This is very delicate to determine numerically. The numerical approaches, polynomial collocation and high-order finite differences, are described in detail in Section 6. We then find that the numerical results and the asymptotic predictions agree very closely when describing the developing singularity, and the change in the solution behaviour as $p \to 5^+$.

1.3. Overview of the analysis

The similarity reduction (2) of the blow-up solutions of the GKdV (1), which will be justified shortly, leads to the following ODE for the function $w(\xi)$:

$$\left(w_{\xi\xi} + w^p\right)_\xi + \frac{1}{3}\left(\frac{2}{p-1}w + \xi w_\xi\right) = 0. \tag{6}$$

It follows from the original PDE (1) that $|w| \to 0$ as $t \to \pm\infty$. A further condition which follows after rescaling the conserved energy (3) is that

$$\int\left(w_\xi^2 - \frac{1}{(p+1)}w^{p+1}\right)d\xi = 0. \tag{7}$$

If $|w| \ll 1$ then (6) reduces to the linear equation

$$w_{\xi\xi\xi} + \frac{1}{3}\left(\frac{2}{p-1}w + \xi w_\xi\right) = 0. \tag{8}$$

Eq. (8) is closely related to the Airy equation. In the limit of $\xi \to -\infty$ it has solutions of the asymptotic form

$$\begin{aligned} w(\xi) \sim\ & A^-|\xi|^{-3/4}e^{-2|\xi|^{3/2}/3\sqrt{3}} + B^-|\xi|^{-3/4}e^{2|\xi|^{3/2}/3\sqrt{3}} \\ & + C^-|\xi|^{-2/(p-1)}. \end{aligned} \tag{9}$$

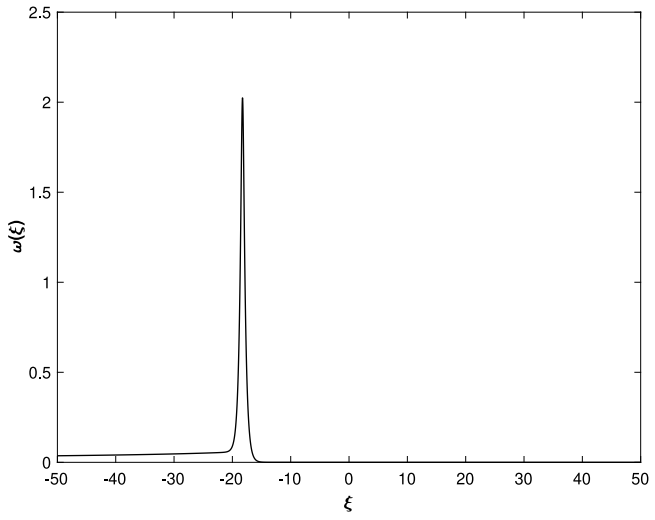

Fig. 1. The form of the rescaled self-similar solution w when $p = 5.1$. In this we can see the sharp peak to the left of the origin, the slow decay as $\xi \to -\infty$ and the more rapid decay as $\xi \to \infty$. Note that this is similar to Fig. 18 in [7].

Similarly, as $\xi \to \infty$ its solutions take the (rapidly oscillating) form

$$w(\xi) \sim A^+ \xi^{-3/4} \cos(2\xi^{3/2}/3\sqrt{3}) + B^+ \xi^{-3/4} \sin(2\xi^{3/2}/3\sqrt{3}) + C^+ |\xi|^{-2/(p-1)}. \tag{10}$$

It follows, by inspection, that to satisfy the integral condition (7) we must have

$$B^- = A^+ = B^+ = 0. \tag{11}$$

Eq. (6) has been studied by a number of authors. In [16,17] it was shown, for $p = 5$, that there exists no solution which also satisfies the condition (7) resp. (10). In contrast when $p > 5$ it was shown rigorously by Koch [19] that a self-similar solution satisfying (7) does exist and that this solution becomes singular in the H^1 norm as $p \to 5$. The key observation is that as $p \to 5$ the height of the solution of the GKdV equation (1) *increases* and the solution peak *moves to* $-\infty$. This is consistent with the fact that no self-similar solution exists for $p = 5$.

In this article, we extend the work in [19] by performing a detailed formal asymptotic analysis of the solution of (6) for $0 < p - 5 \ll 1$ and compare this with very careful numerical calculations. This solution is constructed by considering its form in different regions on the ξ-axis, which are then matched together. First, we examine the solution in the region where w has a peak, we call this the bump region. We then study the solution as it evolves away from the bump, and will find that the behaviour for increasing and decreasing ξ is very different. Finally we match this with the far field behaviour for large $|\xi|$. By doing this we find tight asymptotic results on the scaling of the bump, of the tails and many aspects of the solution, which agree closely with the numerical calculations.

1.4. Summary of the formal asymptotic results

We now summarise the main asymptotic results. The general form of the function $w(\xi)$ is illustrated in Fig. 1 for the value $p = 5.1$. For values of p closer to 5, the shape is similar, but the peak is more pronounced. This solution has a peak at $\xi_{\max} < 0$ with a maximum value of $w_{\max}$, and it decays away from the peak. The decay is slow for $\xi < \xi_{\max}$ and much more rapid for $\xi > \xi_{\max}$.

As described above, for large $|\xi|$ these solutions have algebraic decay with an asymptotic form given by

$$w(\xi) \sim C^{\pm} |\xi|^{-\alpha} \quad \text{as} \quad \xi \to \pm\infty, \text{ where } \alpha = 2/(p-1), \tag{12}$$

so that $\alpha = 1/2$ when $p = 5$. Central to our discussion is the *Ground State Solution* $Q_p(y)$ which satisfies the equation

$$Q_{p,yy} - \frac{Q_p}{3} + Q_p^p = 0, \quad Q_{p,y}(0) = 0, \quad Q_p \to 0 \quad \text{as} \quad |y| \to \infty. \tag{13}$$

This can be found as

$$Q_p(y) = \left(\frac{(p+1)}{6}\right)^{1/(p-1)} \operatorname{sech}^{2/(p-1)}\left(\frac{(p-1)}{2\sqrt{3}} y\right) \tag{14}$$

with, for $p = 5$,

$$Q_5(y) = \operatorname{sech}^{1/2}\left(2y/\sqrt{3}\right). \tag{15}$$

Using formal asymptotic analysis, we obtain the following result

Formal Proposition 1. *Let* $0 < p - 5 \ll 1$.
(i) If $p - 5 \ll 1$ *then the function* $w(\xi)$ *has a sharp peak of width proportional to* $(p-5)^{1/3}$. *Close to the peak (in the 'bump region' of width proportional to* $(p-5)^{1/6}$*) it takes the form of a rescaling of the ground state function* Q_5.
(ii) The value of the maximum and the location of the peak of $w(\xi)$ *are given by*

$$w_{\max} \sim \Lambda^{1/6} (p-5)^{-1/6} \approx 1.4016\,(p-5)^{-1/6},$$
$$\xi_{\max} \sim -\Lambda^{2/3} (p-5)^{-2/3} \approx -3.8591\,(p-5)^{-2/3}, \tag{16}$$

where

$$\Lambda = \frac{\left(\int_{-\infty}^{\infty} Q_5\, dy\right)^2}{\int_{-\infty}^{\infty} Q_5^2\, dy} = \frac{\sqrt{3}\Gamma(1/4)^4}{4\pi^2} = 7.58098\ldots. \tag{17}$$

(iii) In the far field for which $|\xi| \gg 1$ *the function* $w(\xi)$ *takes the form*

$$w(\xi) = C^{\pm} |\xi|^{-2/(p-1)} \quad \text{as} \quad \xi \to \pm\infty, \tag{18}$$

where the constants $C^{\pm}$ *are given by*

$$C^- \approx \left(\frac{\pi\sqrt{3}}{8}\right)^{1/2} (p-5)^{1/2} = 0.8247\,(p-5)^{1/2}, \tag{19}$$

$$C^+ \approx \sqrt{2\Lambda}\,(p-5)^{-1/2} e^{-2\Lambda/3\sqrt{3}(p-5)} = 3.894\,(p-5)^{-1/2} e^{-2.91792/(p-5)}. \tag{20}$$

Note that as $p \to 5$, C_+ is exponentially small and we find that $C_+ \ll C_-$ which explains the asymmetric form of the curve in Fig. 1.

We obtain these results by using asymptotic analysis and matching. Moreover, we will show that there is strong numerical support for all of the conclusions of Formal Proposition 1. The results (16) are similar to those obtained by Koch [19], who also derived the scaling result (17). We will derive this result using a different method, which also gives significant new asymptotic information about the solutions, allowing us to derive the results in (19), (20).

The layout of the remainder of this paper is as follows. In Section 2 we give some important scalings associated with the derivation of (6) and its solution as $p \to 5$. In Sections 3–5 we consider the asymptotic form of this solution for $0 < p - 5 \ll 1$ and derive the results of Formal Proposition 1. In Section 6 we describe the numerical methods used to study (6) in the limit of $p \to 5$. These methods are very delicate as they have to deal with large and singular solutions with (as can be seen from the form of C^+) very rapidly decaying tails. In Section 7 we then compare the numerical results with the asymptotic approximations.

2. Basic scalings and methodology

2.1. Dynamical rescaling

To obtain Eq. (6) from Eq. (1), we assume that the solutions of (1) blow up at a finite time T at the single point $\tilde{x}$ and take a self-similar form. We use the fact that Eq. (1) exhibits the following scaling invariance: if $\phi(x,t)$ is a solution then so is

$$\lambda^{\frac{2}{p-1}}\phi(\lambda x, \lambda^3 t),$$

for every $\lambda > 0$. The solution ansatz (2) follows immediately from this. Furthermore, the energy (3) rewritten in terms of these new variables becomes

$$E(t) = \frac{(T-t)^{-(p+3)/3(p-1)}}{2}\int_{\mathbb{R}}\left[w_\xi^2 - \frac{1}{p+1}w^{p+1}\right]\,d\xi$$

and the mass (4) becomes

$$M(t) = (T-t)^{(p-5)/3}\int_{\mathbb{R}} w^2\,d\xi.$$

Since both $E(t)$ and $M(t)$ must be conserved as $t \to T$ it follows immediately that when $p > 5$, we must have

$$\int_{\mathbb{R}}\left[w_\xi^2 - \frac{1}{p+1}w^{p+1}\right]\,d\xi = 0 \quad \text{and} \quad \int_{\mathbb{R}} w^2\,d\xi = \infty,$$

which is how we obtained condition (7). Therefore, we assume that the function $w(\xi)$ has a bounded H^1 semi-norm and an unbounded L^2 norm. The first condition requires that $w(\xi)$ has non-oscillatory tails, and the second is consistent with tail behaviour of the asymptotic form $w(\xi) \sim 1/|\xi|^{2/(p-1)}$ as in (12).

2.2. Rescaling as $p \to 5$ and a formal asymptotic expansion

We next introduce a rescaling of Eq. (6) which will be needed to derive the asymptotic results. We first introduce the small parameter $0 < \varepsilon \ll 1$ that we use in the asymptotic analysis. In Section 3, we will show that this small parameter arises since a solvability condition at the *first order* of the asymptotic analysis needs to be satisfied. This condition implies that p must be close to $p = 5$, and hence, we introduce

$$\varepsilon = \frac{(p-5)}{\Lambda}, \qquad 0 < \varepsilon \ll 1. \tag{21}$$

Note that to determine the expression (17) for Λ, we even need to go to the *second order* in the asymptotic analysis. As mentioned earlier, this condition was first derived by Koch [19]. We will reestablish it here by using a different method based on matched asymptotic expansions, which also provides a lot of information about the solution. Following [19] we introduce the rescaling

$$v(y) = \varepsilon^{2/3(p-1)}w, \quad y = \varepsilon^{-1/3}\left(\xi + \varepsilon^{-2/3}\right), \tag{22}$$

in Eq. (6) which leads to

$$\begin{aligned}\left(v_{yy} - \frac{v}{3} + v^p\right)_y &= -\frac{\varepsilon}{3}\left(\frac{2v}{(p-1)} + yv_y\right)\\ &= -\frac{\varepsilon}{3}\left(\frac{v}{2} + yv_y\right) + \mathcal{O}\left(\varepsilon^2\right),\end{aligned} \tag{23}$$

with the far-field condition

$$|v| \to 0 \text{ as } y \to \pm\infty \tag{24}$$

In order to fix the phase of the solution, we *assume that the maximum of $v(y)$ (the bump) occurs at $y = 0$ and hence the maximum of $w(\xi)$ occurs at the point $\xi = -\varepsilon^{-2/3} < 0$.* This can be done without loss of generality as it is tied up with the definition of ε which at this stage has a degree of freedom. This phase condition replaces the compatibility condition used in [19].

We study Eq. (23) for v, in various regions on the y-axis. We introduce the so-called *bump region* where $0 \le |y| \ll 1/\sqrt{\varepsilon}$ and for which the leading order of the solution is given by

$$\left(v_{yy} - \frac{v}{3} + v^p\right)_y \approx 0, \quad v(y) \sim Q_p(y).$$

Moreover, we study the solution in the *far field region* where $|y| \gg 1$. In this region, most of the solutions of Eq. (23) are rapidly oscillating and violate (7). In contrast, for those solutions that satisfy the condition (7) and are non-oscillatory, the right-hand side of Eq. (23) is dominant, so that to leading order

$$\frac{2v}{(p-1)} + yv_y \approx 0, \quad v(y) \sim C^{\pm}|y|^{-\frac{2}{p-1}}. \tag{25}$$

Our *formal approach* will be to express $v(y)$ in an asymptotic series of the form

$$v = v_0(y) + \varepsilon v_1(y) + \varepsilon^2 v_2(y) + \cdots \tag{26}$$

in the bump region. In the bump region, we find expressions for $v_0(y)$ and $v_1(y)$ and hence the first terms in the asymptotic solution. The condition for the solvability of the equation for $v_1(y)$, so that $v_1(y)$ does not grow exponentially fast as $|y| \to \infty$, is simply that $p \approx 5$. The condition for the similar solvability of the equation for $v_2(y)$, will lead to the compatibility condition (21). Moreover, we determine an expression for $v_1(y)$ using a variations of constants method. This leads to an expression for the form of the tails of this function $v_1(y)$. We then match these expressions, via an intermediate region, with the non-oscillating solutions of the far field equation in the range $1 \ll |y| \ll 1/\sqrt{\varepsilon}$ to determine the values of $C^{\pm}$.

The *numerical approach* we adopt in Section 6 solves Eq. (23) combined with (25) to eliminate the rapidly oscillating solutions and to find those satisfying (7).

3. The bump region

In this section, we study Eq. (23) in the *bump region* for which

$$\sqrt{\varepsilon}|y| \ll 1. \tag{27}$$

To this end we substitute the asymptotic expansion (26) into Eq. (23) and assume that $\sqrt{\varepsilon}|y| \ll 1$. By comparing the terms of different order in ε we can derive the form of the terms $v_0(y), v_1(y)$ in expression (26) and give a condition for the existence of the function $v_2(y)$. Moreover, we determine the asymptotic form of these solutions as $y \to \pm\infty$ and summarise the resulting expressions in (63) and (64) at the end of this section.

Recall that since we assumed that $y = 0$ is precisely the point where the function $v(y)$ attains its maximum it must satisfy

$$v_y(0) = 0. \tag{28}$$

After substituting expansion (26) into Eq. (23), we collect terms of the same order, see Appendix A for more details. Then, we obtain

Order $\mathcal{O}(\varepsilon^0)$: To leading order we find the equation

$$\begin{aligned}&v_{0,yy} - \frac{v_0}{3} + v_0^p = 0, \quad |v_0| \to 0 \quad \text{as} \quad |y| \to \infty\\ &\text{and} \quad v_{0,y}(0) = 0.\end{aligned} \tag{29}$$

The bounded solution of this equation is given by

$$v_0(y) = Q_p(y) = A\,\text{sech}^{\frac{2}{p-1}}(By), \tag{30}$$

as in expression (14), where we denote

$$A = \left(\frac{p+1}{6}\right)^{\frac{1}{p-1}}, \tag{31}$$

$$B = \frac{p-1}{2\sqrt{3}}, \tag{32}$$

which leads to the expression (15) for $p = 5$. From Eq. (23) we see that this expression is asymptotically valid provided that $\varepsilon|y| \ll 1$. More specifically, we find that for $1 \ll |y| \ll 1/\varepsilon$

$$Q_p(y) = 2^{\frac{2}{p-1}} A e^{-\frac{4}{p-1}B|y|} \quad \text{and} \quad Q_5(y) = \sqrt{2}e^{-|y|/\sqrt{3}}. \tag{33}$$

Rescaling the result (30) back to the original variables w and ξ, by using (21) and (22), we immediately deduce the results in (16). In particular, as $p \to 5$ and $Q_p(y) \to Q_5(y)$ we find that $v(0) \to 1$, and thus, the maximum is given by

$$w_{\max} \to \varepsilon^{-1/6} = \Lambda^{1/6}(p-5)^{-1/6}.$$

Similarly, since $y_{\max} = 0$, we find that it is located at

$$\xi \equiv \xi_{\max} = -\varepsilon^{-2/3} = -\Lambda^{2/3}(p-5)^{-2/3}.$$

Order $\mathcal{O}(\varepsilon)$.: We now collect the order ε terms in Eq. (23). This leads to the following equation for $v_1(y)$:

$$(Lv_1)_y = \left(v_{1,yy} - \frac{1}{3}v_1 + pv_0^{p-1}v_1\right)_y = -\frac{1}{3}\left[\frac{2}{p-1}v_0 + yv_{0,y}\right], \tag{34}$$

$$v_{1,y}(0) = 0.$$

We integrate over y and introduce a constant C so that

$$\begin{aligned} Lv_1 &= v_{1,yy} - \frac{1}{3}v_1 + pv_0^{p-1}v_1 \\ &= -\frac{1}{3}\left[\int_{-\infty}^{y}\left(\frac{2}{p-1}v_0 + sv_{0,s}\right)\,ds + C\right] =: g(y). \end{aligned} \tag{35}$$

Also, we can rewrite the right-hand side as

$$g(y) = -\frac{1}{3}\left[\int_{-\infty}^{y}\frac{3-p}{p-1}v_0\,ds + y\,v_0(y) + C\right], \tag{36}$$

since $|v_0| \to 0$ as $y \to -\infty$.

Observe immediately that the linear operator L has a null eigenfunction $\psi_1(y)$ which decays exponentially at infinity and is given by

$$L\psi_1(y) = 0, \qquad \text{where} \qquad \psi_1 \equiv (v_0)_y = (Q_p)_y. \tag{37}$$

To ensure that v_1 exists, and that it is not exponentially growing at infinity, we apply the Fredholm Alternative. This implies that Eq. (35) has a bounded solution, provided that the right-hand side of this equation $g(y)$ is orthogonal to $\psi_1(y)$. Using integration by parts, it follows that

$$\begin{aligned} &\int_{-\infty}^{\infty}\frac{dv_0}{ds}g(s)\,ds \\ &= -\frac{1}{3}\int_{-\infty}^{\infty}\frac{dv_0}{ds}\left[\int_{-\infty}^{s}\left(\frac{2}{p-1}v_0 + rv_{0,r}\right)\,dr\right]ds \\ &= \frac{1}{3}\int_{-\infty}^{\infty}v_0\left[\frac{2}{p-1}v_0 + sv_{0,s}\right]ds \\ &= -\frac{p-5}{6(p-1)}\int_{-\infty}^{\infty}v_0^2. \end{aligned}$$

Hence, the Fredholm Alternative condition is satisfied at this level of the asymptotic expansion provided that

$$\frac{p-5}{6(p-1)}\int_{-\infty}^{\infty}v_0^2\,ds = \mathcal{O}(\varepsilon),$$

and hence,

$$p - 5 = \mathcal{O}(\varepsilon),$$

since $\int_{-\infty}^{\infty}v_0^2\,ds$ does not become small.

The importance of the critical value of $p = 5$ is now evident. Close to this value we can deduce the existence of a non-exponentially growing solution v_1 of (35).

3.1. Determining the function $v_1(y)$

The Fredholm Alternative guarantees the existence of the function $v_1(y)$. We now determine this solution for $p - 5 = \Lambda\varepsilon$. Moreover, we obtain its asymptotic form in the bump region which is necessary for the later matching arguments. The leading order of Eq. (35) becomes, for $p - 5 = \Lambda\varepsilon$,

$$v_{1,yy} - \frac{1}{3}v_1 + 5v_0^4v_1 = g(y), \tag{38}$$

where g is defined in (36). First, we study the homogeneous part of Eq. (38). As we found before, one solution of this equation is given by

$$\begin{aligned} \psi_1(y) &= v_{0,y} \\ &= -\frac{1}{2}B\,\mathrm{sech}^{\frac{3}{2}}(By)\sinh(By), \end{aligned}$$

where, from (32), $B = 2/\sqrt{3}$ when $p = 5$. This solution is odd and exponentially decaying. Using the method of reduction of order, a second linearly independent solution can be found. We determine it explicitly as

$$\begin{aligned} \psi_2(y) &= \psi_1(y)\int^{y}\frac{ds}{(v_{0,s})^2} \\ &= -\frac{2\left(2\sinh^2(By) - \cosh^2(By)\right)}{B^2\cosh^{\frac{3}{2}}(By)}. \end{aligned}$$

This solution is even and exponentially growing. Finally, the general solution of Eq. (38) can be found by using the method of Variation of Constants. This results in

$$\begin{aligned} v_1(y) &= A_1\,\psi_1(y) + A_2\,\psi_2(y) \\ &\quad - \psi_1(y)\int_0^{y}\psi_2\,g\,ds + \psi_2(y)\int_0^{y}\psi_1\,g\,ds, \end{aligned} \tag{39}$$

where we use that the Wronskian-determinant can be found as

$$\psi_1\frac{d\psi_2}{dy} - \frac{d\psi_1}{dy}\psi_2 = 1.$$

We choose the lower bounds of the integrals in (39) such that these are convenient when determining the integrals. The constants A_1 and A_2 are arbitrary at this stage. However, the phase condition $v_{1,y}(0) = 0$ immediately forces

$$A_1 = 0.$$

3.2. The integrals $\int_0^y \psi_1\,g\,ds$ and $\int_0^y \psi_2\,g\,ds$

In this section we determine the integrals $\int_0^y \psi_1 g\,ds$ and $\int_0^y \psi_2\,g\,ds$ in (39) to obtain an expression for the function $v_1(y)$. Thereafter, we find its asymptotic nature as $|y| \gg 1$ in the next section. We find the first integral as

$$\begin{aligned} &-3\int_0^{y}\psi_1\,g\,ds \\ &= \int_0^{y}v_{0,r}\left[\int_{-\infty}^{r}\left(\frac{1}{2}v_0 + sv_{0,s}\right)\,ds + C\right]dr \\ &= \int_0^{y}v_{0,r}\left(-\frac{1}{2}\int_{-\infty}^{r}v_0\,ds + rv_0 + C\right)dr \end{aligned}$$

$$= -\frac{1}{2}v_0\int_{-\infty}^{y} v_0\,ds + \frac{1}{2}v_0(0)\int_{-\infty}^{0} v_0\,ds + \frac{1}{2}v_0^2 y + C(v_0 - v_0(0)). \tag{40}$$

Next, we determine the second integral given by

$$-3\int_0^y \psi_2\, g\, ds = \int_0^y \psi_2\left[\int_{-\infty}^{r} -\frac{1}{2}v_0\,ds + r v_0(r) + C\right] dr \tag{41}$$

by studying the terms separately. The second and third terms can be found explicitly as

$$J_1 = \int_0^y \psi_2 r v_0(r)\,dr = -\frac{9\log(\cosh(By))}{4} + \frac{3\sqrt{3}y\tanh(By)}{2} - \frac{3y^2}{4} + \frac{9\log(\frac{1}{2})}{4}, \tag{42}$$

and

$$J_2 = \int_0^y \psi_2\,dr = \frac{3\sqrt{3}}{2}\left(\frac{2\sinh(By)}{\sqrt{\cosh(By)}} + 3iE\left(\frac{iy}{\sqrt{3}}\middle|2\right)\right), \tag{43}$$

where E is the incomplete elliptic integral of the second kind, see [20]. The first term in (41) is given by

$$\begin{aligned} J_3 &= -\frac{1}{2}\int_0^y \psi_2\int_{-\infty}^{r} v_0\,ds\,dr \\ &= \frac{9}{16}\int_0^{By}\frac{2\sinh^2(r)-\cosh^2(r)}{\cosh^{\frac{3}{2}} r}\left[\int_{-\infty}^{r}\cosh^{-\frac{1}{2}}(s)\,ds\right] dr \\ &= \frac{9}{16}\left\{4\left(\log(\cosh(By)) - \sinh(By)\cosh^{-\frac{1}{2}}(By)\left(-2iF\left(\frac{iBy}{2}|2\right)\right.\right.\right. \\ &\quad \left.\left.\left. + \frac{\Gamma(\frac{1}{4})^2}{2\sqrt{2\pi}}\right)\right) + 3\int_0^{By}\cosh^{\frac{1}{2}}(r)\left(-2iF\left(\frac{ir}{2}|2\right) + \frac{i\Gamma(\frac{1}{4})^2}{2\sqrt{2\pi}}\right) dr\right\} \\ &= \frac{9}{16}\left\{4\left(\log(\cosh(By)) - \sinh(By)\cosh^{-\frac{1}{2}}(By)\left(-2iF\left(\frac{iBy}{2}|2\right)\right.\right.\right. \\ &\quad \left.\left.\left. + \frac{\Gamma(\frac{1}{4})^2}{2\sqrt{2\pi}}\right)\right) + 3\left(\frac{i\Gamma(\frac{1}{4})^2}{2\sqrt{2\pi}}\left(E\left(\frac{iBy}{2}\middle|2\right) - E\,(0|2)\right)\right. \\ &\quad \left. - 2i\int_0^{By}\cosh^{\frac{1}{2}}(r)F\left(\frac{ir}{2}\middle|2\right) dr\right)\right\}, \end{aligned} \tag{44}$$

where F is the incomplete elliptic integral of the first kind and using the asymptotic expansion of F for $y \to -\infty$. The still unknown term

$$2i\int_0^{By}\cosh^{\frac{1}{2}}(r)F\left(\frac{ir}{2}\middle|2\right) dr$$

cannot be determined explicitly but we can determine its asymptotic form as $y \to \pm\infty$, see Appendix C.

3.3. The asymptotic form of $v_1(y)$ for large $|y|$

Collecting all of the terms in the integrals above and substituting these expressions in the expression (39) for v_1, we obtain that

$$\begin{aligned} v_1(y) = \psi_2(y)\left(A_2 + \frac{1}{3}\left(-\frac{1}{2}v_0\int_{-\infty}^{y} v_0 ds + \frac{1}{2}v_0(0)\int_{-\infty}^{0} v_0 ds\right.\right. \\ \left.\left. + \frac{1}{2}v_0^2 y + C(v_0 - v_0(0))\right)\right) \\ - \frac{1}{3}\psi_1(y)\,(J_1 + J_2 + J_3)\,, \end{aligned} \tag{45}$$

where J_1, J_2 and J_3 are given in (42)–(44), respectively. To match the solution (26) in the bump region to the intermediate solutions, as in Sections 4.2 and 4.3, we need to determine the asymptotic form of $v_1(y)$ for $y \to \pm\infty$. We give the limits of the various terms in Appendix B and here we summarise the results. We find that as $y \to \infty$

$$\begin{aligned} v_1(y) &\to \left(A_2 + \frac{1}{3}v_0(0)\left(\frac{1}{2}\int_{-\infty}^{0} v_0\,ds - C\right)\right)\psi_2(y) + C - \frac{\sqrt{3}\Gamma(\frac{1}{4})^2}{4\sqrt{2\pi}} \\ &\quad + \frac{1}{2}\sqrt{2}\frac{A}{3B^2}ye^{-\frac{y}{\sqrt{3}}} + \frac{\sqrt{6}}{12}y^2 e^{-\frac{y}{\sqrt{3}}}, \end{aligned} \tag{46}$$

and as $y \to -\infty$

$$\begin{aligned} v_1(y) &\to C + \left(A_2 + \frac{1}{3}v_0(0)\left(\frac{1}{2}\int_{-\infty}^{0} v_0\,ds - C\right)\right)\psi_2(y) + \frac{1}{2}\sqrt{2}ye^{-\frac{|y|}{\sqrt{3}}} \\ &\quad - \frac{\sqrt{6}}{12}y^2 e^{-\frac{|y|}{\sqrt{3}}}. \end{aligned} \tag{47}$$

To ensure that $v_1(y)$ is bounded in these limits we need to choose A_2 such that the term multiplying $\psi_2(y)$ is zero as $|y| \to \infty$, since the function $\psi_2(y)$ is exponentially growing. Hence, we choose

$$A_2 = -\frac{1}{3}v_0(0)\left(\frac{1}{2}\int_{-\infty}^{0} v_0\,ds - C\right). \tag{48}$$

Next, from the fact that $v_{1,y}$ must exist (be bounded) for $y \to \pm\infty$, we can determine A_2. For this, we use that from (39), it follows that $v_{1,y} = A_1\psi_{1,y} + A_2\psi_{2,y}$. Then, the fact that ψ_2 is exponentially growing implies that $\lim_{y\to\infty} v_{1,y}$ does not exist *unless* we choose $A_2 = 0$. Therefore, we from now on choose

$$A_2 = 0.$$

This also implies, using expression (48), that we must choose

$$C = \frac{I_1}{2} \equiv \int_{-\infty}^{0} v_0\,ds = \frac{\sqrt{3}\Gamma(\frac{1}{4})^2}{4\sqrt{2\pi}}. \tag{49}$$

This can be summarised as follows,

Proposition 3.1. *It follows that as* $y \to \infty$

$$\begin{aligned} v_1(y) \to \quad & C - \frac{\sqrt{3}\Gamma(\frac{1}{4})^2}{4\sqrt{2\pi}} + \frac{1}{2}\sqrt{2}ye^{-\frac{|y|}{\sqrt{3}}} + \frac{\sqrt{6}}{12}y^2 e^{-\frac{|y|}{\sqrt{3}}} \\ &= \frac{1}{\sqrt{2}}\,y\,e^{-y/\sqrt{3}} + \frac{\sqrt{6}}{12}y^2\,e^{-y/\sqrt{3}}. \end{aligned} \tag{50}$$

Similarly, as $y \to -\infty$

$$v_1(y) \to C + \frac{1}{\sqrt{2}}y\,e^{y/\sqrt{3}} - \frac{\sqrt{6}}{12}y^2\,e^{y/\sqrt{3}}. \tag{51}$$

Remark 3.1. These asymptotic expressions can also be obtained directly by studying Eq. (38) for $v_1(y)$ for $|y| \gg 1$. In the limit of large $|y|$ we can substitute the expression (33) into (38). This gives the following two second order differential equations for $v_1(y)$:

$$v_{1,yy} - \frac{1}{3}v_1 = -\frac{1}{\sqrt{6}}e^{-y/\sqrt{3}} - \frac{\sqrt{2}}{3}y\,e^{-y/\sqrt{3}} - \frac{1}{3}\left(C - \frac{I_1}{2}\right), \quad \text{as} \quad y \to +\infty, \tag{52}$$

$$v_{1,yy} - \frac{1}{3}v_1 = \frac{1}{\sqrt{6}}e^{y/\sqrt{3}} - \frac{\sqrt{2}}{3}y\,e^{y/\sqrt{3}} - \frac{C}{3}, \quad \text{as} \quad y \to -\infty. \tag{53}$$

Both (52) and (53) are simple resonant second order ODEs. Each can be solved directly, leading to the following expressions for

$v_1(y)$ in the asymptotic limits

$$v_1(y) \sim \left(C - \frac{I_1}{2}\right) + \frac{1}{\sqrt{2}}\, y\, e^{-y/\sqrt{3}} + \frac{\sqrt{6}}{12}\, y^2\, e^{-y/\sqrt{3}} \quad \text{as} \quad y \to +\infty, \tag{54}$$

$$v_1(y) \sim C + \frac{1}{\sqrt{2}}\, y\, e^{y/\sqrt{3}} - \frac{\sqrt{6}}{12}\, y^2\, e^{y/\sqrt{3}} \quad \text{as} \quad y \to -\infty. \tag{55}$$

These expressions agree completely with the results of the earlier analysis. Whilst this calculation is very straightforward, the condition $C = I_1/2$ does not follow immediately, although it can be obtained in the matching procedure in Section 4.3. Moreover, the earlier analysis gives an explicit expression for $v_1(y)$ for all y rather than just in the asymptotic limit in this case.

3.4. The solvability condition at $\mathcal{O}(\varepsilon^2)$

To determine an expression for Λ where $(p-5) = \Lambda\varepsilon$ we need to study the terms of $\mathcal{O}(\varepsilon^2)$ of Eq. (23). In this analysis we determine a condition for the existence of the function $v_2(y)$ which directly yields Λ.

Order $\mathcal{O}(\varepsilon^2)$: When we collect the $\mathcal{O}(\varepsilon^2)$ terms in Eq. (23) and integrate over y, we find

$$\begin{aligned} Lv_2 = &-\frac{p(p-1)}{2} v_0^{p-2} v_1^2 - \frac{1}{3}\int_{-\infty}^{y} \left(\frac{v_1}{2} + z v_{1,z}\right)\, dz \\ &+ \frac{\Lambda}{24}\int_{-\infty}^{y} v_0\, dz + \frac{D}{3}, \end{aligned} \tag{56}$$

where D is an integration constant. The solutions to the homogeneous part of this equation are the same as for v_1. As in the case for v_1, it follows from the Fredholm Alternative that for (56) to be soluble for v_2, we require that the right-hand side of the equation is orthogonal to $\psi_1(y) = v_{0,y}$. Accordingly, we require that

$$\begin{aligned} &\frac{p(p-1)}{2}\int_{-\infty}^{\infty} v_0^{p-2} v_1^2 v_{0,y}\, dy = \\ &-\frac{1}{3}\int_{-\infty}^{\infty} v_{0,y}\left(\int_{-\infty}^{y}\left(\frac{2v_1}{(p-1)} + z v_{1,z}\right)\, dz\right) dy \\ &+ \frac{\Lambda}{24}\int_{-\infty}^{\infty} v_{0,y}\left(\int_{-\infty}^{y} v_0\, dz\right)\, dy. \end{aligned}$$

Integrating both sides by parts gives

$$\begin{aligned} -p\int_{-\infty}^{\infty} v_0^{p-1} v_1 v_{1,y}\, dy = &\frac{1}{3}\int_{-\infty}^{\infty}\left(\frac{2v_0 v_1}{p-1} + y v_0 v_{1,y}\right)\, dy \\ &- \frac{\Lambda}{24}\int_{-\infty}^{\infty} v_0^2\, dy. \end{aligned} \tag{57}$$

Next, we use Eq. (35) and multiply this by the function $v_{1,y}$. After integrating by parts from $-\infty$ to ∞, we obtain the identity

$$\begin{aligned} &\frac{1}{2}\left[v_{1,y}^2\right]_{-\infty}^{\infty} - \frac{1}{6}\left[v_1^2\right]_{-\infty}^{\infty} + p\int_{-\infty}^{\infty} v_0^{p-1} v_1 v_{1,y}\, dy \\ &= -\frac{1}{3}\int_{-\infty}^{\infty}\left((p-3)\frac{v_0 v_1}{p-1} + y v_0 v_{1,y}\right) dy \\ &\quad -\frac{C}{3}\left[v_1\right]_{-\infty}^{\infty} + \frac{p-3}{3(p-1)}\lim_{y\to\infty} v_1 \int_{-\infty}^{\infty} v_0\, dz. \end{aligned} \tag{58}$$

Then, we add the above two equations, (57) and (58), use that $\lim_{y\to\infty} v_1 = C - I_1/2 = 0$, (50) and apply integration by parts, to obtain

$$\begin{aligned} &\frac{1}{2}\left[v_{1,y}^2\right]_{-\infty}^{\infty} - \frac{1}{6}\left[v_1^2\right]_{-\infty}^{\infty} \\ &= \frac{5-p}{3(p-1)}\int_{-\infty}^{\infty} v_0 v_1\, dy - \frac{\Lambda}{24}\int_{-\infty}^{\infty} v_0^2\, dy - \frac{C}{3}\left[v_1\right]_{-\infty}^{\infty} \\ &\quad + \frac{p-3}{3(p-1)}(C - \frac{I_1}{2})\int_{-\infty}^{\infty} v_0 dz = -\frac{\Lambda}{24}\int_{-\infty}^{\infty} v_0^2\, dy - \frac{C}{3}\left[v_1\right]_{-\infty}^{\infty}. \end{aligned}$$

This is satisfied, and hence v_2 will exist, provided that Λ is given by the identity

$$\frac{\Lambda}{4} = \frac{\left[v_1^2\right]_{-\infty}^{\infty} - 2C\left[v_1\right]_{-\infty}^{\infty}}{I_2} - 3\left[v_{1,y}^2\right]_{-\infty}^{\infty}, \tag{59}$$

where

$$I_2 \equiv \int_{-\infty}^{\infty} v_0^2\, dy = \frac{\pi\sqrt{3}}{2}. \tag{60}$$

It is immediate from the expressions (50) and (51) that

$$\left[v_{1,y}^2\right]_{-\infty}^{\infty} = 0.$$

Moreover, from these expressions it also follows that

$$\begin{aligned} &\left[v_1^2\right]_{-\infty}^{\infty} = (C - \frac{I_1}{2})^2 - C^2 = -\frac{I_1^2}{4}, \qquad \text{and hence,} \\ &\left[v_1\right]_{-\infty}^{\infty} = -\frac{I_1}{2}, \\ &\left[v_1^2\right]_{-\infty}^{\infty} - 2C\left[v_1\right]_{-\infty}^{\infty} = \frac{I_1^2}{4}, \end{aligned} \tag{61}$$

where we use the result $C = I_1/2$ that we obtained at order ε, see (49). Thus, combining (59) and (61) we find that

$$\Lambda = \frac{I_1^2}{I_2}, \tag{62}$$

which gives the results stated in (17).

We summarise the analysis of the bump region $|y| \ll 1/\varepsilon$ as follows. We have found the existence of the function $v_2(y)$, provided that Λ satisfies (62), and hence, the existence of the first three terms of an asymptotic expansion of the solution v of the form of (26). If $1 \ll |y| \ll 1/\sqrt{\varepsilon}$ the resulting solution has the asymptotic expressions

$$\begin{aligned} &v(y) \\ &= \sqrt{2}e^{-y/\sqrt{3}} + \varepsilon\, y\left(\frac{1}{\sqrt{2}} + \frac{\sqrt{6}}{12}\, y\right) e^{-y/\sqrt{3}} + \varepsilon^2\, v_2(y) + \mathcal{O}\left(\varepsilon^3\right), \end{aligned} \tag{63}$$

as $y \to \infty$, and

$$v(y) = \sqrt{2}e^{y/\sqrt{3}} + \varepsilon\, y\left(\frac{1}{\sqrt{2}} - \frac{\sqrt{6}}{12}\, y\right) e^{y/\sqrt{3}} + \varepsilon^2\, v_2(y) + \mathcal{O}\left(\varepsilon^3\right) \tag{64}$$

as $y \to -\infty$. We now proceed to match to the far field. Note that whilst we needed to show the existence of the function $v_2(y)$, we do not actually need to determine it to perform the matching analysis.

4. The mid-range solution and its far field limit

4.1. Overview

So far, we found that the general form of the solution in the bump region is comprised of a peak with exponential decay away from the peak. We now consider the problem (23) given by

$$\begin{aligned} \left(v_{yy} - \frac{v}{3} + v^p\right)_y &= -\frac{\varepsilon}{3}\left(\frac{2v}{(p-1)} + y v_y\right) \\ &= -\frac{\varepsilon}{3}\left(\frac{v}{2} + y v_y\right) + \mathcal{O}\left(\varepsilon^2\right), \end{aligned}$$

in the region where $\sqrt{\varepsilon}|y|$ is no longer small. In this case the solution can be expressed in terms of combinations of multiples of Airy functions. The allowed combination is dictated by the strong requirement that the solution should satisfy the integral condition (7) and also by the need to match to the solution in the bump region.

Using the boundary condition (24), we can assume that the term of the form v^p in Eq. (23) is small and the far field equation becomes to leading order

$$v_{yyy} + \frac{1}{3}(\varepsilon y - 1)v_y + \frac{\varepsilon}{6}v = 0. \tag{65}$$

It can be seen that the solutions to this equation have a different form for $\varepsilon y > 1$ than when $\varepsilon y < 1$. To make this clear, we introduce a rescaled variable

$$z = 12^{-1/3}\varepsilon^{1/3}\left(\varepsilon^{-1} - y\right) = 12^{-1/3}\varepsilon^{-\frac{2}{3}}\left(1 - \varepsilon y\right). \tag{66}$$

Using this rescaling, Eq. (65) becomes the third order equation

$$v_{zzz} - 4zv_z - 2v = 0, \tag{67}$$

which has a *turning point* at $z = 0$ i.e. at $y = 1/\varepsilon$. The general solution of (67) is well known to be a linear combination of $A_i^2(z), A_i(z)B_i(z)$ and $B_i^2(z)$ where $A_i(z)$ and $B_i(z)$ are the *Airy Functions*. Due to the turning point behaviour, the two cases of $z > 0$ and $z < 0$ differ so we will consider them separately.

4.2. The solution when $y < 0$ and $z > 0$

In the region where $y < 0$ and $z > 0$ we write the solution as

$$v(z) = c_0A_i^2(z) + c_1A_i(z)B_i(z) + c_2B_i^2(z), \tag{68}$$

where c_0, c_1 and c_2 are constants that will be chosen in the matching procedure.

Proposition 4.1. *The solution (68) exactly matches that in the bump region provided that*

$$c_0 = 4\pi\, 12^{-1/6}\sqrt{2}\ \varepsilon^{-1/3}e^{\frac{2}{3\sqrt{3}\varepsilon}}, \quad c_1 = C\ 2\pi\, 12^{-1/6}\ \varepsilon^{2/3}, \quad c_2 = 0. \tag{69}$$

Proof. In the case when $z \gg 1$ it is well known that the combinations of the Airy functions take the following asymptotic forms, all of which are non-oscillatory:

$$A_i^2(z) \sim \frac{1}{4\pi z^{1/2}}e^{-\frac{4}{3}z^{3/2}}, \quad B_i^2(z) \sim \frac{1}{\pi z^{1/2}}e^{\frac{4}{3}z^{3/2}}, \quad A_i(z)B_i(z) \sim \frac{1}{2\pi z^{1/2}}. \tag{70}$$

Next, we rewrite these asymptotic expressions in terms of y by using the relation (66) which also implies that

$$z^{3/2} = \frac{1}{12^{1/2}}\varepsilon^{-1}(1 - \varepsilon y)^{3/2}.$$

We will consider the matching range of $1 \ll |y| \ll 1/\sqrt{\varepsilon}$ to that $\sqrt{\varepsilon}|y| \ll 1$. Therefore, it follows that

$$z^{3/2} = \frac{1}{2\sqrt{3}}\varepsilon^{-1} - \frac{\sqrt{3}}{4}y + \varepsilon\frac{\sqrt{3}}{16}y^2 + \mathcal{O}(\varepsilon^2). \tag{71}$$

Furthermore, we use

$$(1 - \varepsilon y)^{-1/2} = 1 + \frac{1}{2}\varepsilon y + \mathcal{O}(\varepsilon^2)$$

to express the asymptotic form of the combined Airy functions in this range as

$$A_i^2(y) = \frac{12^{1/6}}{4\pi}\varepsilon^{1/3}e^{-\frac{2}{3\sqrt{3}\varepsilon}}e^{y/\sqrt{3}}(1 - \varepsilon\frac{\sqrt{3}}{3}y^2 + \mathcal{O}(\varepsilon^2)) \times (1 + \frac{1}{2}\varepsilon y + \mathcal{O}(\varepsilon^2)), \tag{72}$$

$$B_i^2(y) = \frac{12^{1/6}}{\pi}\varepsilon^{1/3}e^{\frac{2}{3\sqrt{3}\varepsilon}}e^{-y/\sqrt{3}}(1 + \varepsilon\frac{\sqrt{3}}{3}y^2 + \mathcal{O}(\varepsilon^2)) \times (1 + \frac{1}{2}\varepsilon y + \mathcal{O}(\varepsilon^2)), \tag{73}$$

$$A_i(y)B_i(y) = \frac{12^{1/6}}{2\pi}\varepsilon^{1/3}(1 + \frac{1}{2}\varepsilon y + \mathcal{O}(\varepsilon^2)). \tag{74}$$

We now match the solution (68) to the solution in the bump region for $y < 0$ and $|y| \gg 1$. From the expression (30) for v_0 and the asymptotic expression for v_1 (51), we find in this range that

$$v(y) = v_0(y) + \varepsilon v_1(y) + \cdots = \sqrt{2}e^{y/\sqrt{3}} + \varepsilon\left(C + \frac{1}{2}\sqrt{2}ye^{y/\sqrt{3}} - \frac{1}{2\sqrt{6}}y^2e^{y/\sqrt{3}}\right) + \cdots \tag{75}$$

Therefore, we can match solution (68), using (72)–(74) with the expression (75) provided that

$$c_0 = 4\pi\, 12^{-1/6}\sqrt{2}\ \varepsilon^{-1/3}e^{\frac{2}{3\sqrt{3}\varepsilon}}, \quad c_1 = C\ 2\pi\, 12^{-1/6}\ \varepsilon^{2/3}, \quad c_2 = 0, \tag{76}$$

such that solution (68) becomes

$$v(y) = c_0A_i^2(y) + c_1A_i(y)B_i(y) = \sqrt{2}\ e^{y/\sqrt{3}}\left(1 + \varepsilon\left(\frac{1}{2}y - \frac{y^2}{4\sqrt{3}}\right)\right) + \varepsilon\ C. \tag{77}$$

After rearranging, this is exactly the same as expression (75). □

Observe that this leads to a solution with both exponentially and polynomially decaying terms. We can summarise the results as follows.

Proposition 4.2. *(i) As $y \to -\infty$, for $|y| \gg 1/\varepsilon$ the solution of (23) is polynomially decaying and has the form*

$$v(y) = \frac{\varepsilon C}{(1 - \varepsilon y)^{1/2}} \sim \frac{C\varepsilon^{1/2}}{(-y)^{1/2}}. \tag{78}$$

Rewritten in terms of the original variables this takes the form

$$w(\xi) = \frac{C\varepsilon^{1/2}}{(-\xi)^{1/2}}, \quad \xi \to -\infty. \tag{79}$$

(ii) This solution satisfies the integral condition (7).

Proof. Using that in (69) we find that $c_2 = 0$ and substituting this into (68), it follows that $v(z) = c_0A_i^2(z) + c_1A_i(z)B_i(z)$ as $\xi \to -\infty$. When $|y| \gg 1/\varepsilon$, the contribution of the A_i^2 term to this solution becomes exponentially small, and hence, only the polynomially decaying solution

$$v(z) = c_1A_1(z)B_1(z) = 12^{-1/6}\epsilon^{2/3}C/z^{1/2}$$

remains. Rescaling using expression (66) gives

$$v(y) = \frac{C\epsilon}{(1 - \epsilon y)^{1/2}}.$$

In terms of the original variables we have

$$1 - \epsilon y = -\epsilon^{2/3}\xi.$$

The result for $w(\xi)$ follows directly. A further direct calculation shows that this far field solution satisfies the integral condition. □

4.3. The solution when $y > 0$

In the region where $y > 0$, we write the solution as the following linear combination of products of Airy functions:

$$v(z) = d_0 A_i^2(z) + d_1 A_i(z)B_i(z) + d_2 B_i^2(z). \tag{80}$$

Proposition 4.3. *The solution of the form (80) matches with the bump region solution and also satisfies the integral condition (7) provided that*

$$d_1 = 0, \quad \text{and} \quad d_0 = d_2 = \frac{\pi\sqrt{2}\varepsilon^{-1/3}}{12^{1/6}} e^{-\frac{2}{3\sqrt{3}\varepsilon}}. \tag{81}$$

Proof. When $y > 0$ and $y \ll 1$, we have two regimes: the **first** when $y \ll 1/\varepsilon$, with $z > 0$ and $z \gg 1$, and the **second** when $y \gg 1/\varepsilon$, with $z < 0$ and $|z| \gg 1$. In the first regime the combined Airy functions have the exponential/polynomial asymptotic form as in (72)–(74). In contrast, in the second regime where $z < 0$ and $|z| \gg 1$ the Airy solutions have the following forms which are highly oscillating

$$\begin{aligned}
A_i^2(z) &= \frac{1}{\pi}|z|^{-1/2}\sin^2(2|z|^{3/2}/3 + \pi/4),\\
B_i^2(z) &= \frac{1}{\pi}|z|^{-1/2}\cos^2(2|z|^{3/2}/3 + \pi/4),\\
A_i(z)B_i(z) &= \frac{1}{\pi}|z|^{-1/2}\sin(2|z|^{3/2}/3 + \pi/4)\cos(2|z|^{3/2}/3 + \pi/4).
\end{aligned} \tag{82}$$

We note that a general linear combination of these functions will be *rapidly oscillating*. If we consider, for example, the function $f(x) = \sin^2(x^{3/2})/\sqrt{x}$ it is evident that its derivative $f_x(x) = \mathcal{O}(1)$ and does not decay as $x \to \infty$, whereas the function $f(x)^6 = \mathcal{O}(1/x^3)$ decays rapidly. Thus any (highly oscillatory) function of this general form will violate the integral condition (7). However, there exists one special linear combination of the products of the Airy functions which does not lead to oscillating solutions and decays as $1/|z|^{1/2}$ and hence satisfies the integral condition (7). This is given by choosing

$$d_0 = d_2 \quad \text{and} \quad d_1 = 0, \tag{83}$$

giving part of (81).

The value of d_0 (and hence of d_2) will be now obtained by a matching argument. First, we match the above solutions in the first regime (when $0 \ll y \ll 1/\sqrt{\varepsilon}$ and also $z > 0$ and $z \gg 1$) to the solution in the bump region. It follows from (83), (72) and (73) that this solution (80) takes the form

$$\begin{aligned}
&v(y)\\
&= d_0(A_i^2 + B_i^2)\\
&= d_0\tfrac{12^{1/6}}{\pi}\varepsilon^{1/3}\Big(\tfrac{1}{4}e^{-\frac{2}{3\sqrt{3}\varepsilon}}e^{y/\sqrt{3}}(1 - \varepsilon\tfrac{\sqrt{3}}{3}y^2 + \mathcal{O}(\varepsilon^2))(1\\
&\quad + \tfrac{1}{2}\varepsilon y + \mathcal{O}(\varepsilon^2))\\
&\quad + e^{\frac{2}{3\sqrt{3}\varepsilon}}e^{-y/\sqrt{3}}(1 + \varepsilon\tfrac{\sqrt{3}}{3}y^2 + \mathcal{O}(\varepsilon^2))(1 + \frac{1}{2}\varepsilon y + \mathcal{O}(\varepsilon^2))\Big).
\end{aligned} \tag{84}$$

In the same range the solution $v(y)$ in the bump region takes the form

$$v(y) = \sqrt{2}e^{-y/\sqrt{3}} + \varepsilon\left(\tfrac{1}{2}\sqrt{2}ye^{-y/\sqrt{3}} + \tfrac{1}{2\sqrt{6}}y^2e^{-y/\sqrt{3}}\right). \tag{85}$$

Note that the first term in (84) is exponentially small since $y \ll 1/\sqrt{\varepsilon}$. Now, if

$$d_0 = \tfrac{\pi\sqrt{2}\varepsilon^{-1/3}}{12^{1/6}}e^{-\frac{2}{3\sqrt{3}\varepsilon}}, \tag{86}$$

then (84) takes the form

$$v(y) = \sqrt{2}\,e^{-y/\sqrt{3}}\left(1 + \varepsilon\left(\tfrac{1}{2}y + \tfrac{y^2}{4\sqrt{3}}\right)\right) \tag{87}$$

which matches to (85). This gives the second relation in (81) and completes the proof. □

We can now determine the form of the solution (80) for $y \to \infty$ (and $|y| \gg 1/\sqrt{\varepsilon}$). This is given by

$$\begin{aligned}
v(y) &= \frac{1}{\pi}d_0|z|^{-1/2}\\
&= \frac{\pi\sqrt{2}\varepsilon^{-1/3}12^{-1/6}}{\pi\,12^{-1/6}\varepsilon^{1/6}y^{1/2}}e^{-\frac{2}{3\sqrt{3}\varepsilon}} \sim \sqrt{2}\varepsilon^{-1/2}e^{-\frac{2}{3\sqrt{3}\varepsilon}}y^{-1/2}.
\end{aligned} \tag{88}$$

Rescaling as before to give the solution in terms of the original variables $p - 5$, w and ξ we find that

$$w(\xi) \sim \sqrt{2}\Lambda^{1/2}(p-5)^{-1/2}e^{-\frac{2\Lambda}{3\sqrt{3}(p-5)}}\xi^{-1/2}. \tag{89}$$

5. The far field region

In the far field region where $|y| \gg 1$ the right-hand side of Eq. (23) is dominant so that the leading order solution satisfies

$$\frac{2v}{p-1} + yv_y = 0, \tag{90}$$

and hence, to leading order

$$v(y) = C^{\pm}|y|^{\frac{2}{p-1}},$$

for $y \to \pm\infty$. Next, rewriting this in terms of the original variables and using that $p = 5 + \mathcal{O}(\varepsilon)$, this solution becomes for $|\xi| \gg 1$ and $\xi < 0$

$$w(\xi) = \frac{C^-}{(-\xi)^{1/2}}, \quad \xi \to -\infty. \tag{91}$$

This solution corresponds to expression (79) when we choose

$$\begin{aligned}
C^- &= \varepsilon C = \varepsilon^{1/2}I_1/2 = \frac{I_1}{2\Lambda^{1/2}}(p-5)^{1/2} = \frac{I_2^{1/2}}{2}(p-5)^{1/2}\\
&= 0.8247\ldots(p-5)^{1/2},
\end{aligned} \tag{92}$$

where we use that we showed in Section 3.3, (49), that $C = I_1/2$ and the fact that $\varepsilon = \frac{p-5}{\Lambda}$. This gives the result (19).

The solution to (90) for $|\xi| \gg 1$ and $\xi > 0$ is given in terms of the original variables as

$$w(\xi) = \frac{C^+}{\xi^{1/2}}, \quad \xi \to \infty, \tag{93}$$

which is the same as expression (89) when we choose

$$\begin{aligned}
C^+ &= \sqrt{2}\Lambda^{1/2}(p-5)^{-1/2}e^{-\frac{2\Lambda}{3\sqrt{3}(p-5)}}\\
&= 3.894(p-5)^{-1/2}e^{-2.91792/(p-5)}.
\end{aligned} \tag{94}$$

This yields the result in (20).

6. Numerical approach

We now present a set of numerical calculations of the solution of Eq. (6) as $p \to 5$. This is a delicate calculation as we have to consider solutions defined on the whole real line, which also vary rapidly over a small interval, see Fig. 1, where the solution is plotted for the value $p = 5.1$. In this section, we describe the numerical methods that are used. In particular we describe the use of polynomial collocation methods and finite difference schemes.

6.1. Polynomial collocation (PolColl)

Our first numerical approach is polynomial collocation. The MATLAB™ software package `bvpsuite1.1` [21] is designed to solve implicit nonlinear boundary value problems (BVPs) in ODEs and differential algebraic equations. The solver routine is based on a class of polynomial collocation methods whose orders may vary from 2 to 8. Collocation has been investigated in the context of singular differential equations of first and second order in [22–24], respectively and this method is shown to be robust with respect to *singularities in the independent variable* and retains its high convergence order in case that the analytical solution is appropriately smooth. The code also provides an asymptotically correct estimate for the global error of the numerical approximation. To enhance the efficiency of the method, a mesh adaptation strategy is implemented, which attempts to choose grids related to the solution behaviour, in such a way that the tolerance is satisfied with the least possible effort. The error estimation procedure and the mesh adaptation work dependably provided that the solution of the problem and its global error are appropriately smooth.[1] The code and the manual can be downloaded from http://www.math.tuwien.ac.at/~ewa. For further information see [21]. This software proved useful for the approximation of numerous singular BVPs important for applications, see e.g. [25–28]. Possible alternative solution methods are given by the MATLAB standard codes `bvp4c` and `bvp5c`. The reasons to use our own code are the following: The mentioned standard codes are written for nonlinear first order systems of ODEs . This implies the need to transform the KdV equation of order three to three equations of order one, which unnecessarily enlarges the dimension of the problem. `bvpsuite` can approximate the third order formulation directly. We have demonstrated in earlier work [27,29] that the numerical solution of boundary value problems of higher order may provide advantages with respect to computation time and accuracy over the approach of transforming to a first order problem before numerical approximation. Moreover, the order of the methods implemented in `bvp4c` and `bvp5c` is fixed at 4 and 5, respectively. In `bvpsuite`, we choose the order automatically in relation to the prescribed user tolerance to optimise effort and efficiency. The order of the collocation executed on equidistant collocation points varies from 2 to 8, on Gaussian points from 4 to 16. These are advantages the above standard MATLAB codes do not provide.

To more precisely describe the collocation approach used in `bvpsuite1.1`, we consider the problem

$$f(x, y(x), y'(x), y''(x), y'''(x)) = 0, \quad x \in [a, b], \tag{95}$$

subject to three boundary conditions,

$$b(y(0), y'(0), y''(0), y(1), y'(1), y''(1)) = 0. \tag{96}$$

We first choose $k \in \mathbb{N}$ and discretise problem (95)–(96). To this end, the interval of integration $[a, b]$ is partitioned as

$$\Delta := \{a = x_0 < x_1 < \cdots < x_{I-1} < x_I = b\},$$

and in each subinterval $[x_j, x_{j+1}]$ we introduce k collocation nodes $x_{jl} := x_j + u_l h_j$, $h_j = x_{j+1} - x_j$, $j = 0, \ldots, I-1$, $l = 1, \ldots, k$, where $0 < u_1 < \cdots < u_k < 1$.[2] By $\mathcal{P}_{k,\Delta}$, we denote the class of piecewise polynomial functions which are *globally* in $C^2[a, b]$ and reduce in each subinterval $[x_j, x_{j+1}]$ to a polynomial p_j of degree less than or equal to $k + 2$. We now approximate the analytical solution y by a polynomial function $p \in \mathcal{P}_{k,\Delta}$, such that p satisfies the system (95) at the collocation points,

$$f(x_{jl}, p(x_{jl}), p'(x_{jl}), p''(x_{jl}), p'''(x_{jl})) = 0, \quad l = 1, \ldots, k, \quad j = 0, \ldots, I-1,$$

the boundary conditions

$$b(p(0), p'(0), p''(0), p(1), p'(1), p''(1)) = 0,$$

and the continuity relations,

$$p_{j-1}(x_j) = p_j(x_j), \quad p'_{j-1}(x_j) = p'_j(x_j), \quad p''_{j-1}(x_j) = p''_j(x_j), \quad j = 1, \ldots, I-1,$$

where $p(x) := p_j(x)$, $x \in [x_j, x_{j+1}]$. Inspecting the number of unknowns and the number of equations, we easily see that the discrete system is closed.

6.1.1. Adaptive mesh selection

The mesh selection strategy implemented in `bvpsuite` was proposed and investigated in [30]. Most modern mesh generation techniques in two-point boundary value problems construct a smooth function mapping a uniform auxiliary grid to the desired nonuniform grid. In [30] a new system of control algorithms for constructing a grid density function $\phi(x)$ is described. The local mesh width $h_i = x_{i+1} - x_i$ is computed as $h_i = \epsilon_N / \varphi_{i+1/2}$, where $\epsilon_N = 1/N$ is the accuracy control parameter corresponding to N subintervals, and the positive sequence $\Phi = \{\varphi_{i+1/2}\}_{i=0}^{N-1}$ is a discrete approximation to the continuous density function $\phi(x)$, representing the mesh width variation. Using an error estimate, a feedback control law generates a new density from the previous one. Digital filters may be employed to process the error estimate as well as the density [31].

6.2. Finite difference schemes (FDS)

The second algorithm used for the numerical simulations is the MATLAB™ code `HoFiD_UP` [32] . This solver is based on finite difference schemes whose order is even and varies from 4 to 8, and can solve kth order ODE systems including those of the form (95), subject to general nonlinear boundary conditions. The main idea of the algorithm is to discretise each derivative separately by means of high order finite differences with a variable number of initial/final values. Again we use the grid Δ and denote the approximations to the exact solution by $y_i \approx y(x_i)$, $i = 0, 1, \ldots, n$. Then the $r + s$ steps formula approximating the ν-th derivative in the grid point x_i is given by

$$y^{(\nu)}(x_i) \approx y_i^{\nu} = \frac{1}{h_i^{\nu}} \sum_{j=-s}^{r} \alpha_{s+j}^{(s,\nu)} y_{i+j}.$$

This formula includes s values of y on the left-hand side of y_i, r values of y on the right-hand side of y_i and y_i itself. The coefficients $\alpha_{s+j}^{(s,\nu)}$ are computed to obtain the maximal order of consistency, $q = r + s + 1 - \nu$ and depend on the ratio of the interval lengths in two consecutive blocks. Popular choices for r are $r = s - 1$ or $r = s$. For more details see the discussion of the boundary value methods (BVMs) in [33]. In `HoFiD_UP` an adaptive step control technique is utilised which aims at the equidistribution of the local error (residual). The error is estimated using the deferred correction technique involving two consecutive even order schemes [34]. Moreover, the variable mesh consists of blocks of at least $q + 4$ equidistant points each, so that the whole grid is piecewise constant. For stiff ODEs, or singularly perturbed problems with very small perturbation parameters, order variation and continuation strategies are implemented. The order of the method is then chosen

[1] The required smoothness of higher derivatives is related to the order of the used collocation method.

[2] The values $u_1 = 0$ and $u_k = 1$ are excluded to avoid the evaluation at possibly singular points located at the boundaries of the interval $[a, b]$.

Table 1
Change in the solution characteristics with integration interval $[-L, L]$.

L	$w(-6)$	$w(0)$	$\|w\|_\infty$
10	0.8059	0.0501	1.3515
20	0.8054	0.0501	1.3515
30	0.8055	0.0501	1.3515
40	0.8055	0.0501	1.3515
50	0.8055	0.0501	1.3515

depending on the tolerances and for nonlinear problems the continuation strategy is applied. Experimental results show that, in general, the grids from `HoFiD_UP` are coarser when compared with other available software [32]. The efficiency and robustness of the above schemes has been illustrated in the context of singular eigenvalue Sturm–Liouville problems [35], the porous medium equation [36], and multi-parameter BVPs with singular points [37].

7. Numerical simulations

We now apply the methods described in the previous section to Eq. (6). To ensure that we only find those algebraically decaying solutions which are not highly oscillating, and are thus consistent with the conditions (7), (9), (10) we require that the solutions should satisfy the asymptotic boundary conditions

$$\frac{2}{(p-1)}w(\xi)+\xi w_\xi(\xi)\xrightarrow{\xi\to\pm\infty}0, \qquad w_{\xi\xi}(\xi)\xrightarrow{\xi\to\infty}0. \tag{97}$$

We solve this system by using both numerical methods specified in Section 6 independently. In particular, we determine the maximum of the soluton, its location and the tail behaviour of the solution. We show that the results of the numerical calculations agree closely with the predictions of Proposition 1.

7.1. Problem setting and numerical results for $p = 6$

We solve the problem (6), (97) on a finite interval $(-L, L)$ with a sufficiently large L. This method is appropriate as the solution decays fairly rapidly for $L \to \infty$ and consequently, the length L can be chosen to be not too large. Accordingly we replace the boundary condition (97) with the finite domain condition:

$$\begin{aligned}&\frac{2}{(p-1)}w(-L)-Lw_\xi(-L)=0,\\ &\frac{2}{(p-1)}w(L)+Lw_\xi(L)=0, \quad w_{\xi\xi}(L)=0.\end{aligned} \tag{98}$$

7.1.1. Convergence orders and plots of the numerical solutions

We illustrate the behaviour of adaptive collocation methods for the relatively moderate value of $p = 6$. There, it was found by varying L that $L = 30$ is sufficient,[3] since on larger intervals the values $w(-6)$, $w(0)$ and $\|w\|_\infty$ no longer change with L, see Table 1. Since according to the results, enlarging L beyond $L = 30$ has almost no influence, we fix $L = 30$ for the asymptotic simulations based on PolColl, which are reported in Section 7.2.1. The reliability of the computations is demonstrated by the convergence orders documented in Table 2, which are calculated empirically for collocation at two resp. three equidistant and two Gaussian collocation points, where the errors are calculated by comparison with a precise reference solution.

[3] However, for p closer to 5, the simulations require a larger interval, see Section 7.2.2.

Table 2
PolColl: Errors 'err_*' and convergence orders ('ord') of collocation at two and three equidistant collocation points ('e2' resp. 'e3') as well as of collocation at two Gaussian points ('g2'). The results are computed for $L = 10$.

h	err_{e2}	ord	err_{e3}	ord	err_{g2}	ord
1/50	$1.8600e-02$	–	$1.1300e-02$	–	$1.6601e-05$	–
1/100	$2.6000e-03$	2.86	$1.9915e-05$	9.15	$3.2406e-05$	−0.97
1/200	$6.5774e-04$	2.00	$1.2560e-06$	3.99	$2.0160e-06$	4.01
1/400	$1.6427e-04$	2.00	$7.8684e-08$	4.00	$1.2554e-07$	4.01
1/800	$4.1061e-05$	2.00	$4.9202e-09$	4.00	$7.8396e-09$	4.00

7.1.2. Solving the problem for $p = 6$ with the adaptive mesh option

Next, we solve the problem with $p = 6$ using `bvpsuite1.1` as described in Section 6.1 in conjunction with mesh adaptation in order to observe if the meshes correctly reflect the solution behaviour. Similar results are obtained using the FDS method described in Section 6.2. For the absolute and relative tolerances $TOL_a = TOL_r = 10^{-4}$, the results can be found in Fig. 2. The problem was solved using collocation at one Gaussian point and $L = 20$. We denote by M_i the number of subintervals in the equidistant initial mesh, M_f is the number of subintervals in the final mesh chosen by our adaptive mesh selection procedure. Fig. 2 shows for $M_i = 3200$ a typical location of the mesh points which become denser in the region where the solution changes rapidly. In the figure, we only show 40 mesh points out of $M_f = 3333$ points. Typically, the number of mesh points in the final mesh does not depend on M_i in case that M_i is sufficiently large to provide dependable information on the solution structure. If M_i is too large, the code may reduce the number of mesh points. The rather dense mesh is due to the low method order, rough solution behaviour and required long interval of integration. In the next run, we choose two Gaussian collocation points and reduce M_i to $M_i = 100$. Then, we require $M_f = 558$ to satisfy the tolerance with an estimated error of 1.1796×10^{-5}. If we move to three Gaussian points and start with $M_i = 67$, then the code provides a solution whose estimated error is $3.9856e-6$ with $M_f = 264$. In all three cases, the values of $w(-6)$, $w(0)$ and $\|w\|_\infty$ are the same and correct within the prescribed tolerance.

7.2. The solution behaviour for p varying from $p = 6$ to $p = 5$

7.2.1. Behaviour close to the peak

Having established the reliability of the numerical method, we now decrease the value of p from 6 to 5 to allow a comparison with the asymptotic results. As $p \to 5$ we expect a far more pronounced (almost) singular peak in the solution, and thus the adaptivity will be essential. We use `bvpsuite` to solve (6), (98) for each p specified in Fig. 3, which illustrates the behaviour of the peak in $w(\xi)$ as $p \to 5$. In Table 3, we collect data describing the change in the solutions while p decays from 6 to 5, the location $\xi_{\max}$ of the maximum in column two, the value of the maximum $w(\xi_{\max})$, see column three (illustrated in Fig. 3, and the norms $\|w\|^2_{L^2}$, $\|w'\|^2_{L^2}$, $\|w\|^2_{H^1}$ in columns four, five, and six,[4] respectively.

Now, we will compare the results from the numerical simulations with those of the asymptotic analysis as summarised in Proposition 1. We first study the solution close to the peak. In Fig. 4 (left) we present a log–log plot of $w(\xi_{\max})$ plotted as a function of $p - 5$. We plot the numerical values of $w(\xi_{\max})$ in

[4] To compute the H^1-norm of $w(\xi)$, we use approximation by a sum of eight Gaussian functions,

$$w(\xi)\approx\sum_{i=1}^{8}a_i\exp\left(-\left(\frac{\xi-b_i}{c_i}\right)^2\right),\ a_i,b_i,c_i\in\mathbb{R}.$$

M_i	M_f	err_{abs}
200	3332	$1.0189e-04$
400	3332	$1.0189e-04$
800	3332	$1.0189e-04$
1600	3332	$1.0189e-04$
3200	3332	$1.0189e-04$

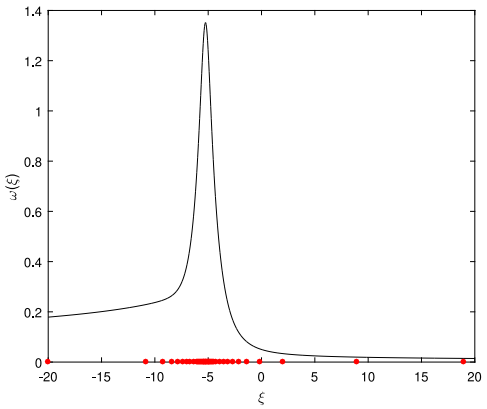

Fig. 2. Solution of Eq. (6) using the PolColl method with $TOL_a = TOL_r = 10^{-4}$ and $L = 20$.

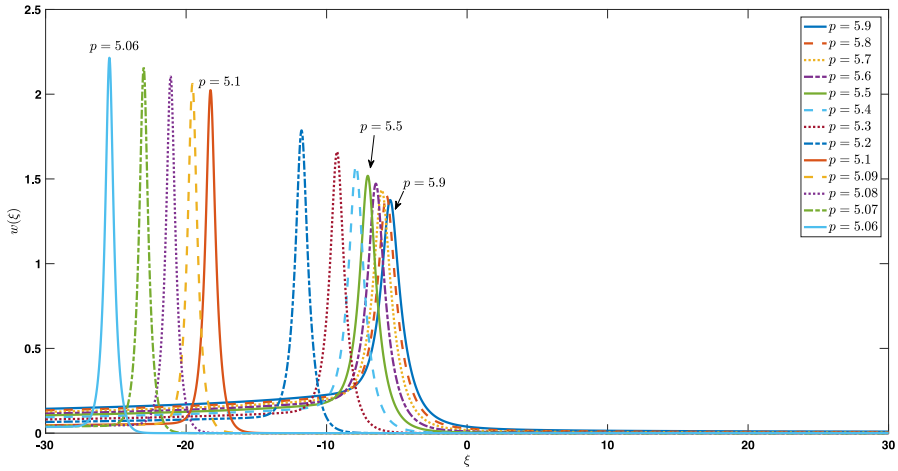

Fig. 3. PolColl: Numerical solutions $w(\xi)$ obtained by collocation at one Gaussian point for varying values of $5 < p < 6$. In this plot we see the peak of the solution $w(\xi)$ moving to the left, and becoming more singular, as $p \to 5^+$.

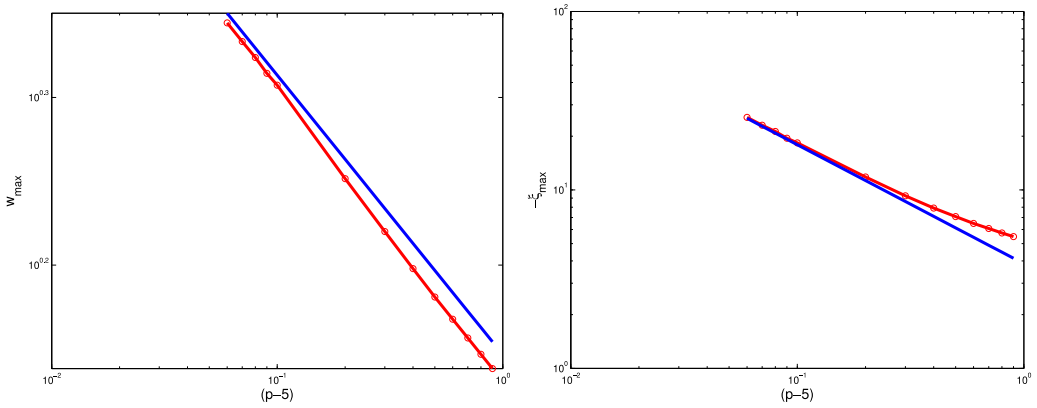

Fig. 4. Left: PolColl: Log–log plot of $w(\xi_{\max})$ as a function of $p-5$ obtained from the numerical simulations (red dotted line) compared to the asymptotic approximation (blue), Right: PolColl: Log–log plot of $-\xi_{\max}$ as a function of $p-5$ obtained from the numerical simulations (red dotted line) compared to the asymptotic approximation (blue). (For interpretation of the references to colour in this figure legend, the reader is referred to the web version of this article.)

red, and in blue the approximation from (16). In Fig. 4 (right) we similarly present a log–log plot of $-\xi_{\max}$ plotted as a function of $p-5$, comparing the numerical (red) and theoretical approximation given in (16). Both plots in Fig. 4 show a convergence of the numerical calculations to the asymptotic estimate as p approaches $p = 5$ and give convincing evidence for their accuracy. Recall that the asymptotic analysis is performed for p close to $p = 5$. We conclude that the numerical calculations strongly support the asymptotic estimates for the behaviour of the peak.

7.2.2. Behaviour in the solution tails

We now consider the asymptotic behaviour of the tails of the function $w(\xi)$ as $\xi \to \pm\infty$ and $p \to 5$ for which the approximations are given in (12) with (19), (20). To obtain a

Table 3
PolColl: Characteristic data for $w(\xi)$, $5.06 \le p \le 5.90$, $\xi \in [-30, 30]$.

p	$\xi_{\max}$	$w(\xi_{\max})$	$\|w\|^2_{L^2}$	$\|w'\|^2_{L^2}$	$\|w\|^2_{H^1}$
5.9	−5.4750	1.3750	3.3853	1.5448	4.9301
5.8	−5.7375	1.4022	3.2745	1.6892	4.9637
5.7	−6.0750	1.4339	3.1752	1.8634	5.0386
5.6	−6.4875	1.4713	3.0735	2.0911	5.1646
5.5	−7.0875	1.5168	2.9831	2.3778	5.3609
5.4	−7.9125	1.5773	2.8905	2.8139	5.7044
5.3	−9.2625	1.6597	2.8135	3.4660	6.2795
5.2	−11.8125	1.7846	2.7295	4.6628	7.3923
5.10	−18.3375	2.0291	2.6941	7.6880	10.3821
5.09	−19.4875	2.0625	2.6928	8.2956	10.9884
5.08	−21.2625	2.1078	2.6909	9.0208	11.7117
5.07	−23.0437	2.1545	2.6761	9.8819	12.5580
5.06	−25.4812	2.2105	2.6186	10.9553	13.6369

Table 4
Starting values from FDS, final step with PolColl: Coefficients of the function $f(\xi) = a \cdot (-\xi)^b$ for $\xi \to -\infty$ and $g(\xi) = c \cdot \xi^d$ for $\xi \to \infty$.

p	a	b	c	d	$-2/(p-1)$
5.100	0.2457	−0.4878	1.125e − 12	−0.4877	−0.4878
5.095	0.2400	−0.4884	2.499e − 13	−0.4883	−0.4884
5.090	0.2342	−0.4890	4.681e − 14	−0.4889	−0.4890
5.085	0.2281	−0.4896	7.205e − 15	−0.4895	−0.4896
5.080	0.2219	−0.4902	8.745e − 16	−0.4901	−0.4902
5.075	0.2154	−0.4908	7.957e − 17	−0.4907	−0.4908
5.070	0.2086	−0.4914	5.142e − 18	−0.4913	−0.4914
5.065	0.2015	−0.4920	2.173e − 19	−0.4919	−0.4920
5.060	0.1942	−0.4926	5.376e − 21	−0.4925	−0.4926
5.055	0.1864	−0.4932	6.807e − 23	−0.4931	−0.4932
5.050	0.1782	−0.4938	3.548e − 25	−0.4937	−0.4938
5.045	0.1695	−0.4944	5.730e − 28	−0.4944	−0.4944
5.040	0.1603	−0.4951	1.826e − 31	−0.4950	−0.4950
5.035	0.1504	−0.4957	5.719e − 36	−0.4956	−0.4957
5.030	0.1396	−0.4963	5.411e − 42	−0.4962	−0.4963
5.025	0.1278	−0.4969	1.813e − 50	−0.4968	−0.4969
5.020	0.1144	−0.4975	2.370e − 63	−0.4974	−0.4975
5.015	0.0987	−0.4981	7.311e − 86	−0.4980	−0.4981

numerical estimate we assume the ansatz that the solution has the following form

$$w(\xi) = a \cdot (-\xi)^b \quad \text{for} \quad \xi \to -\infty \quad \text{and}$$
$$w(\xi) = c \cdot \xi^d \quad \text{for} \quad \xi \to \infty.$$

The values of a, b, c, d are then estimated by fitting this ansatz to the numerical solution data. Using the FDS method of Section 6.2, we were able to cover the interesting range close to $p = 5.0$, see Table 4 for p between $p = 5.1$ and $p = 5.015$. As a starting guess, solution values from a FDS of order 6 with constant stepsize $h = 0.01$ have been used. The values of the approximate solution were provided from the FDS on the intervals $[\xi_{\max} - 350, \xi_{\max} + 50]$ and $[\xi_{\max} - 50, \xi_{\max} + 350]$. Thereafter, we applied the PolColl method to provide the solution values in the required intervals $[\xi_{\max} - 1030, \xi_{\max} - 30]$ for $\xi \to -\infty$ and $[\xi_{\max} + 30, \xi_{\max} + 1030]$ for $\xi \to +\infty$. As a first observation, these results show a perfect agreement between the estimates of b, d and the asymptotic estimate of $-2/(p-1)$ given in (12). It is also very clear that $a \gg c$. Indeed the values of c are extremely small and to determine them is an arbitrative test for the numerical method.

Behaviour as $\xi \to -\infty$.

Now, we compare the numerically obtained value of a with the theoretical approximation in (19) which gives that $a = C^- = 0.8247\ (p-5)^{1/2}$. To examine this estimate in Fig. 5 we plot $a/(p-5)^{1/2}$ as a function of $(p-5)$ (on a linear scale) and include the value of 0.8247. We see that, apart from what appears to be a loss of numerical accuracy for the smallest value of $p-5$, there is strong support for the asymptotic estimate.

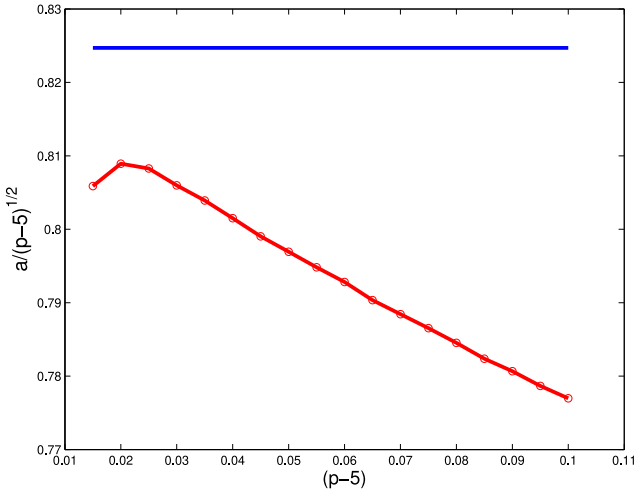

Fig. 5. The function $a/(p-5)^{1/2}$ plotted as a function of $p-5$ (red dotted line) together with the asymptotic limit of 0.8247 (blue). (For interpretation of the references to colour in this figure legend, the reader is referred to the web version of this article.)

Behaviour as $\xi \to \infty$.

In the numerical estimate, we have observed that $c \to 0$ very rapidly as $p \to 5$. This is consistent with the estimate

$$c = C^+ = 3.894\ (p-5)^{-1/2}\ e^{-2.91792/(p-5)}$$

in (20) As a first check of this estimate in Fig. 6 (left) we plot $\log(c)$ as a function of $1/(p-5)$. We note that this graph is (as expected) close to linear with an estimated gradient close to the predicted value of −2.9172. As a more refined calculation, in Fig. 6 (right) we give a log–log plot of c as a function of $p-5$ in red, and compare with the asymptotic approximation in blue. Again, apart from the results for $p-5$ very close to zero, we have excellent agreement between the asymptotic and numerical estimates over a huge range of values assumed by c. We conclude that the behaviour in the tails of the numerically calculated solution is close to that found in the asymptotic analysis.

8. Conclusions

The formal asymptotic analysis presented here has clearly shown the nature of the similarity solution when $p > 5$ and the manner in which the similarity solution becomes singular as $p \to 5^+$. It has given detailed information about the solution which agrees closely with the results of some very careful numerical calculations. This gives us confidence in the use of both approaches to studying the blow-up solutions.

Acknowledgements

The authors thank Stefan Schirnhofer, former student at Vienna University of Technology, for the numerical computations performed with the polynomial collocation code `bvpsuite`.

Appendix A. Derivation of the inner expansion equations

Consider Eq. (23)

$$\left(v_{yy} - \frac{v}{3} + v^p\right)_y = -\frac{\epsilon}{3}\left(\frac{2v}{(p-1)} + y v_y\right). \tag{A.1}$$

Now substitute into (A.1) the asymptotic expression (26)

$$v(y) = v_0(y) + \epsilon v_1(y) + \epsilon^2 v_2(y) + \cdots.$$

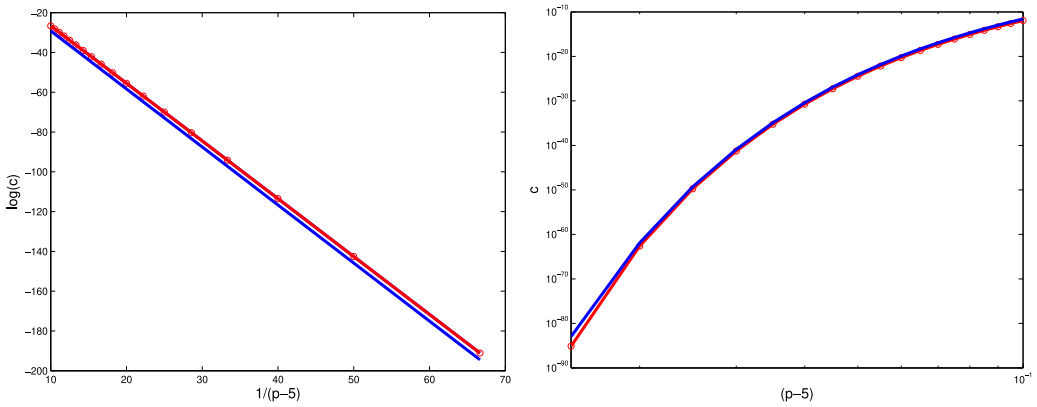

Fig. 6. Left: The values of $\log(c)$ plotted as a function of $1/(p-5)$ (red dotted line) and the line $-2.9172/(p-5)$ (blue). Right: A log–log plot of c plotted as a function of $(p-5)$ (red dotted line) compared with the asymptotic estimate (blue). (For interpretation of the references to colour in this figure legend, the reader is referred to the web version of this article.)

It is clear that the left-hand side of (A.1) then becomes:

$$\left(v_{0,yy}-\frac{v_0}{3}+v_0^p\right)_y+\epsilon\,(L\,v_1)_y \\ +\epsilon^2\left(L\,v_2+\frac{p(p-1)}{2}v_0^{p-2}v_1\right)_y+\cdots \tag{A.2}$$

where

$$Lv\equiv v_{yy}-\frac{v}{3}+v_0^p v.$$

If we take

$$p-5=\Lambda\epsilon$$

then

$$\frac{2}{(p-1)}=\frac{1}{2}-\frac{\Lambda\epsilon}{8}+\cdots$$

It follows that the right-hand side of (A.1) becomes

$$-\epsilon\left(\frac{v_0}{6}+\frac{yv_{0,y}}{3}\right)-\epsilon^2\left(\frac{v_1}{6}-\frac{\Lambda v_0}{24}+\frac{yv_{1,y}}{3}\right)+\cdots \tag{A.3}$$

Collecting terms at the different orders of ϵ and integrating with respect to y, gives the respective Eqs. (28), (33) and (55).

Appendix B. The asymptotic behaviour of the function $v_1(y)$

In this appendix, we determine the asymptotic expansions for the terms in the expression (45) for $v_1(y)$ as $y\to\pm\infty$. We start with the first term in (45) by first determining the asymptotics of $\int_0^y\psi_1 g\,ds$, (40). As $y\to\infty$ we have

$$-3\int_{-\infty}^{y}\psi_1 g\,ds=\left(\frac{1}{2}\int_{-\infty}^{0}v_0\,ds-C\right)v_0(0) \\ +\,v_0\left(-\frac{1}{2}\int_{-\infty}^{\infty}v_0\,ds+\frac{1}{2}v_0 y+C\right).$$

Similarly, as $y\to-\infty$

$$-3\int_{-\infty}^{y}\psi_1 g\,ds=\left(\frac{1}{2}\int_{-\infty}^{0}v_0\,ds-C\right)v_0(0)+\left(\frac{1}{2}v_0 y+C\right)v_0.$$

We now multiply by the function $\psi_2(y)$ and use the result that $\psi_2(y)v_0(y)\to-2/B^2=-3/2$, as $y\to\pm\infty$, to deduce that as $y\to\infty$

$$-3\psi_2(y)\int_{-\infty}^{y}\psi_1 g\,ds=\psi_2(y)v_0(0)\left(\frac{1}{2}\int_{-\infty}^{0}v_0\,ds-C\right) \\ -\frac{3}{4}\left(-\int_{-\infty}^{\infty}v_0\,ds+y\,v_0(y)+2C\right).$$

Similarly, as $y\to-\infty$ we have

$$-3\psi_2(y)\int_{-\infty}^{y}\psi_1 g\,ds \\ =\psi_2(y)v_0(0)\left(\frac{1}{2}\int_{-\infty}^{0}v_0\,ds-C\right)-\frac{3}{4}\left(y\,v_0(y)+2C\right).$$

Next, we determine the leading order of the other terms of the form $\psi_1(y)\,(J_1+J_2+J_3)$ in the expression (45) for $v_1(y)$, where we use the identities (42)–(44). We find that

$$\psi_1(y)J_1\to\pm\frac{1}{2}\sqrt{2}\frac{A}{B}y^2e^{\frac{-B|y|}{2}}$$

as $y\to\pm\infty$. Similarly, as $y\to\pm\infty$,

$$\psi_1(y)J_2\to\mp\frac{1}{2}\sqrt{2}ABe^{\frac{-B|y|}{2}}\frac{\frac{8\sinh(By)}{\sqrt{\cosh(By)}}+12iE\left(\frac{iBy}{2}\middle|2\right)}{AB^3} \\ =\frac{1}{2B^2}(8-12)=-\frac{2}{B^2}.$$

Now, we determine the leading order form of $\psi_1(y)J_3$ by splitting J_3 in (44) into two terms. The first term, multiplied by $\psi_1(y)$, is given to leading order by

$$\frac{4\psi_1(y)}{B^4}\left(\log(\cosh(By))-\sinh(By)\cosh^{-\frac{1}{2}}(By) \right. \\ \left.\times\int_{-\infty}^{By}\cosh^{-\frac{1}{2}}(w)\,dw\right) \\ =\frac{4\psi_1(y)}{B^4}\left(\log(\cosh(By))-\sinh(By)\cosh^{-\frac{1}{2}}(By)\left(-2iF\left(\frac{iBy}{2}|2\right)\right.\right. \\ \left.\left.+\frac{\Gamma(\frac{1}{4})^2}{2\sqrt{2\pi}}\right)\right) \\ =\frac{4\psi_1(y)}{B^4}\left(\frac{By}{2}+\frac{\Gamma(\frac{1}{4})^2}{4\sqrt{\pi}}e^{\frac{By}{2}}\right) \\ =A\frac{\sqrt{2}\Gamma(\frac{1}{4})^2}{B^3\sqrt{\pi}}+\sqrt{2}\frac{A}{B^2}ye^{-\frac{1}{2}By},$$

for $y\to\infty$. Similarly, if $y\to-\infty$

$$\frac{4\psi_1}{B^4}\left(\log(\cosh(By))-\sinh(By)\cosh^{-\frac{1}{2}}(By)\int_{-\infty}^{By}\cosh^{-\frac{1}{2}}(w)dwdr\right) \\ =\sqrt{2}\frac{A}{B^2}ye^{-\frac{1}{2}B|y|}.$$

The second term in J_3 can be found by using the result that

$$\begin{aligned}
&\int_0^{By} \cosh^{\frac{1}{2}}(r)\left(-2iF\left(\frac{ir}{2}|2\right)+\frac{i\Gamma(\frac{1}{4})^2}{2\sqrt{2\pi}}\right)dr\\
&=-2i\int_0^{By}\cosh^{\frac{1}{2}}(r)F\left(\frac{ir}{2}\middle|2\right)dr\\
&\quad+\frac{i\Gamma(\frac{1}{4})^2}{2\sqrt{2\pi}}\left(E\left(\frac{iBy}{2}\middle|2\right)-E\left(0|2\right)\right)\\
&=\int_0^{By}\cosh^{\frac{1}{2}}(r)F\left(\frac{ir}{2}\middle|2\right)dr-\frac{i\Gamma(\frac{1}{4})^2}{4\sqrt{\pi}}e^{\frac{By}{2}}.
\end{aligned}\tag{B.1}$$

Here, F is the incomplete elliptic integral of the first kind and we use the asymptotic expansion of F for $y\to-\infty$. The still unknown term

$$2i\int_0^{By}\cosh^{\frac{1}{2}}(r)F\left(\frac{ir}{2}\middle|2\right)dr,$$

cannot be determined explicitly, but we determine its asymptotic form as $y\to\pm\infty$ in Appendix C.

Multiplying (B.1) by $\psi_1(y)$, this yields

$$\begin{aligned}
&\frac{3\psi_1}{B^4}\int_0^{By}\cosh^{\frac{1}{2}}(r)\left(-2iF\left(\frac{ir}{2}\middle|2\right)+\frac{i\Gamma(\frac{1}{4})^2}{2\sqrt{2\pi}}\right)dr\\
&=\frac{3\psi_1\Gamma(\frac{1}{4})^2}{\sqrt{2\pi}B^4}e^{\frac{By}{2}}=-\frac{3\Gamma(\frac{1}{4})^2}{\sqrt{2\pi}B^3},
\end{aligned}\tag{B.2}$$

for $y\to\infty$, and

$$\frac{3\psi_1}{B^4}\int_0^{By}\cosh^{\frac{1}{2}}(r)\int_{-\infty}^{r}\cosh^{-\frac{1}{2}}(w)\,dw\,dr=0,$$

for $y\to-\infty$.

Summarising, as $y\to\infty$

$$\psi_1(y)J_3\to-\frac{A}{2B^3}\frac{\Gamma(\frac{1}{4})^2}{\sqrt{2\pi}}-\sqrt{2}\frac{A}{B^2}ye^{-\frac{1}{2}By},$$

and as $y\to-\infty$,

$$\psi_1J_3\to\sqrt{2}\frac{A}{B^2}ye^{-\frac{1}{2}B|y|}.$$

Therefore, collecting all the above we find that as $y\to\infty$

$$-3\psi_1(y)\int_0^{y}\psi_2 g\,dr\to-\frac{A}{B^3}\frac{\Gamma(\frac{1}{4})^2}{\sqrt{2\pi}}+C\frac{2}{B^2}+\frac{\sqrt{2}A}{B^2}ye^{-\frac{1}{2}By},\tag{B.3}$$

and as $y\to-\infty$

$$-3\psi_1(y)\int_0^{y}\psi_2 g\,dr\to C\frac{2}{B^2}+\frac{\sqrt{2}A}{B^2}ye^{-\frac{1}{2}B|y|}.$$

Finally, substituting all these results into (39) we find the asymptotic expansions for $v_1(y)$ given in (46) and (47).

Appendix C. The asymptotic expansion of $\int_0^{By}\cosh^{\frac{1}{2}}(r)F\left(\frac{ir}{2}\middle|2\right)dr$

We determine the asymptotics of the integral $\int_0^{By}\cosh^{\frac{1}{2}}(r)F\left(\frac{ir}{2}\middle|2\right)dr$ by splitting the integral, using the fact that the function $2iF\left(\frac{ir}{2}\middle|2\right)$ is odd and bounded. Therefore, we can split the integral such that the first part is constant and the second part can be determined by using the asymptotic limit of $2iF\left(\frac{ir}{2}\middle|2\right)$. First, we study the region $y>0$. Introducing the value $1\ll y_0<y$, we rewrite the integral as

$$2i\int_0^{By}\cosh^{\frac{1}{2}}(r)F\left(\frac{ir}{2}\middle|2\right)dr\tag{C.1}$$

$$\begin{aligned}
&=2i\left\{\int_0^{By_0}\cosh^{\frac{1}{2}}(r)F\left(\frac{ir}{2}\middle|2\right)dr\right.\\
&\quad\left.+\int_{By_0}^{By}\cosh^{\frac{1}{2}}(r)F\left(\frac{ir}{2}\middle|2\right)dr\right\}\\
&=2i\left\{iC_1+\int_{By_0}^{By}\cosh^{\frac{1}{2}}(r)F\left(\frac{ir}{2}\middle|2\right)dr\right\}\\
&=2i\left\{iC_1+\lim_{w\to\infty}F\left(\frac{iw}{2}\middle|2\right)\int_{By_0}^{By}\cosh^{\frac{1}{2}}(r)\,dr\right\},
\end{aligned}$$

for some constant C_1. Next, we use the results that the integral of $\cosh^{\frac{1}{2}}(r)$ can be determined explicitly as the incomplete integral of the second kind E, and that the asymptotic expressions of both F and E are known. We deduce that as $y\to\infty$

$$\begin{aligned}
&2i\int_0^{By}\cosh^{\frac{1}{2}}(r)F\left(\frac{ir}{2}\middle|2\right)dr\\
&=2i\left\{iC_1-2i\lim_{w\to\infty}F\left(\frac{iw}{2}\middle|2\right)\left(E\left(\frac{iBy}{2}\middle|2\right)\right.\right.\\
&\quad\left.\left.-E\left(\frac{iBy_0}{2}\middle|2\right)\right)\right\}\\
&=-4\lim_{w\to\infty}F\left(\frac{iw}{2}\middle|2\right)E\left(\frac{iBy}{2}\middle|2\right)+\text{h.o.t.}\\
&=-4i\frac{\Gamma(\frac{1}{4})^2}{4\sqrt{2\pi}}\frac{i}{\sqrt{2}}e^{\frac{By}{2}}+\text{h.o.t.}\\
&=\frac{\Gamma(\frac{1}{4})^2}{2\sqrt{\pi}}e^{\frac{By}{2}}.
\end{aligned}\tag{C.-1}$$

For $y<0$, we determine the integral by transforming the integration variable by setting $r=-s$ which leads to

$$2i\int_0^{By}\cosh^{\frac{1}{2}}(r)F\left(\frac{ir}{2}\middle|2\right)dr=2i\int_0^{-By}\cosh^{\frac{1}{2}}(s)F\left(\frac{is}{2}\middle|2\right)ds.$$

Therefore, by using the above asymptotic expressions as $y\to\infty$, we find that

$$2i\int_0^{By}\cosh^{\frac{1}{2}}(r)F\left(\frac{ir}{2}\middle|2\right)dr=\frac{(\Gamma(\frac{1}{4}))^2}{2\sqrt{\pi}}e^{\frac{B|y|}{2}}+\text{h.o.t.}$$

as $y\to-\infty$.

References

[1] Y. Lan, Stable self-similar blow-up dynamics for slightly l^2-supercritical generalized KDV equations, Comm. Math. Phys. 345 (2016) 223–269.

[2] T. Benjamin, Lectures on nonlinear wave motion, in: Lectures in Applied Math, vol. 15, AMS, 1974.

[3] T. Benjamin, J. Bona, J. Mahoney, Model equations for long wave nonlinear dispersive media, Philos. Trans. R. Soc. Lond. Ser. A 272 (1971) 47–78.

[4] N. Zabusky, Fermi, Pasta, Ulam, solitons and the fabric of nonlinear and computational science: History, synergetics, and visiometrics, Chaos 15 (2005).

[5] D. Korteweg, G. de Vries, On the change of form of long waves advancing in a rectangular canal, and on a new type of long stationary waves, Phil. Mag. 5 (39) (1895) 422–443.

[6] M. Ablowitz, M. Kruskal, H. Segur, A note on Miura's transformation, J. Math. Phys. 20 (1979) 999–1003.

[7] C. Klein, R. Peter, Numerical study of blow-up and dispersive shocks in solutions to generalised Korteweg–de Vries equations, Physica D 305 (2015) 52–78.

[8] P.D. Lax, Integrals of nonlinear equations of evolution and solitary waves, Comm. Pure Appl. Math. 21 (1968) 467–490, http://dx.doi.org/10.1002/cpa.3160210503/abstract.

[9] R. Miura, The Korteweg-de Vries equation: A survey of results, SIAM Rev. 18 (3) (1976) 412–459, http://www.jstor.org/stable/2028638.

[10] R. Pego, M. Weinstein, Asymptotic stability of solitary waves, Comm. Math. Phys. 164 (1994) 305–349.

[11] J.L. Bona, P.E. Souganidis, W.A. Strauss, Stability and instability of solitary waves of Korteweg-de Vries type, Proc. R. Soc. Lond. Ser. A Math. Phys. Eng. Sci. 411 (1841) (1987) 395–412, arXiv:http://rspa.royalsocietypublishing.org/content/411/1841/395full.pdf+html, http://rspa.royalsocietypublishing.org/content/411/1841/395abstract.
[12] J. Bona, V. Dougalis, O. Karakashian, W. McKinney, Conservative high-order numerical schemes for the generalized Korteweg-de Vries equation, Philos. Trans. R. Soc. Lond. Ser. A 351 (1995) 107–164.
[13] D.B. Dix, W.R. McKinney, Computations of self-similar blow-up solutions of the generalized Korteweg-de Vries equation, Differential Integral Equations 11 (1998) 679–723.
[14] Y. Martel, F. Merle, A Liouville theorem for the critical generalized Korteweg-de Vries equation, J. Math. Pures Appl. (9) 79 (2000) 339–425.
[15] Y. Martel, F. Merle, Instability of solitons for the critical generalized Korteweg-de Vries equation, Geom. Funct. Anal. 11 (2001) 74–123.
[16] F. Merle, Existence of blow-up solutions in the energy space for the critical generalized KdV equation, J. Amer. Math. Soc. 14 (2001) 555–578, http://www.ams.org/journals/jams/2001-14-03/S0894-0347-01-00369-1/.
[17] Y. Martel, F. Merle, Blow up in finite time and dynamics of blow up solutions for the l^2-critical generalized KdV equation, J. Amer. Math. Soc. 15 (2002) 617–664, http://www.ams.org/journals/jams/2002-15-03/S0894-0347-02-00392-2/.
[18] Y. Martel, F. Merle, Stability of blow-up profile and lower bounds for blow-up rate for the critical generalized KdV equation, Ann. Math. 155 (1) (2002) 235–280, http://www.jstor.org/stable/3062156.
[19] H. Koch, Self-similar solutions to super-critical gKdV, Nonlinearity 28 (2015) 545–575.
[20] M. Abramowitz, I.A. Stegun, Handbook of Mathematical Functions with Formulas, Graphs, and Mathematical Tables, Dover, New York, 1964.
[21] G. Kitzhofer, G. Pulverer, C. Simon, O. Koch, E. Weinmüller, The new MATLAB solver bvpsuite for the solution of singular implicit BVPs, JNAIAM J. Numer. Anal. Ind. Appl. Math. 5 (2010) 113–134.
[22] F. de Hoog, R. Weiss, Collocation methods for singular boundary value problems, SIAM J. Numer. Anal. 15 (1978) 198–217.
[23] O. Koch, Asymptotically correct error estimation for collocation methods applied to singular boundary value problems, Numer. Math. 101 (2005) 143–164.
[24] E. Weinmüller, Collocation for singular boundary value problems of second order, SIAM J. Numer. Anal. 23 (1986) 1062–1095.
[25] C. Budd, O. Koch, E. Weinmüller, From nonlinear PDEs to singular ODEs, Appl. Numer. Math. 56 (2006) 413–422.
[26] R. Hammerling, O. Koch, C. Simon, E. Weinmüller, Numerical solution of singular ODE eigenvalue problems in electronic structure computations, J. Comput. Phys. 181 (2010) 1557–1561.
[27] G. Kitzhofer, O. Koch, P. Lima, E. Weinmüller, Efficient numerical solution of the density profile equation in hydrodynamics, J. Sci. Comput. 32 (2007) 411–424.
[28] I. Rachunkova, G. Pulverer, E. Weinmüller, A unified approach to singular problems arising in the membrane theory, Appl. Math. 55 (2010) 47–75.
[29] J. Cash, G. Kitzhofer, O. Koch, G. Moore, E. Weinmüller, Numerical solution of singular two-point BVPs, JNAIAM J. Numer. Anal. Ind. Appl. Math. 4 (2009) 129–149.
[30] G. Pulverer, G. Söderlind, E. Weinmüller, Automatic grid control in adaptive BVP solvers, Numer. Algorithms 56 (1) (2011) 61–92.
[31] G. Söderlind, Digital filters in adaptive time-stepping, ACM Trans. Math. Softw. 29 (2003) 1–26.
[32] P. Amodio, G. Settanni, A finite differences MATLAB code for the numerical solution of second order singular perturbation problems, J. Comput. Appl. Math. 236 (2012) 3869–3879.
[33] P. Amodio, I. Sgura, High order generalized upwind schemes and numerical solution of singular perturbation problems, BIT 47 (2007) 241–257.
[34] P. Amodio, G. Settanni, A deferred correction approach to the solution of singularly perturbed BVPs by high order upwind methods: implementation details, in: T. Simos, G. Psihoyios, C. Tsitouras (Eds.), AIP Conference Proceedings: Numerical analysis and applied mathematics - ICNAAM 2009, vol. 1168, 2009, pp. 711–714.
[35] P. Amodio, G. Settanni, Variable-step finite difference schemes for the solution of Sturm-Liouville problems, Commun. Nonlinear Sci. Numer. Simul. 20 (2015) 41–649.
[36] P. Amodio, C. Budd, O. Koch, G. Settanni, E. Weinmüller, Asymptotical computations for a model of flow in saturated porous media, Appl. Math. Comput. 237 (2014) 155–167.
[37] P. Amodio, T. Levitina, G. Settanni, E. Weinmüller, Numerical simulation of the whispering gallery modes in prolate spheroids, Comput. Phys. Comm. 185 (2014) 1200–1206.